Supporting Information

Breaking the Heavy-Atom Paradigm: Weak-Donor-Engineered Triplet Harvesting in BODIPY Photosensitizers for Immunogenic Pyroptosis Therapy

Hyeong Seok Kim,[1,2+] Hyeonji Rha,[1+] Mohammad Izadyar,[3,5+] Supphachok Chanmungkalakul,[3] Haiqiao Huang,[4] Yi Young Kang,[2] Jae-Won Ka,[2] Yunjie Xu,[1*] Mingle Li,[4*] Xiaogang Liu,[3*] and Jong Seung Kim[1*]

Affiliations

[1] Department of Chemistry, Korea University, Seoul, 02841, Korea

[2] Advanced Functional Polymers Research Center, Korea Research Institute of Chemical Technology, Daejeon, 34114, Korea.

[3] Fluorescence Research Group, Singapore University of Technology and Design, 487372, Singapore

[4] College of Materials Science and Engineering, Shenzhen University, Shenzhen, 518060, China

[5] Research Center for Modeling and Computational Sciences, Faculty of Science, Ferdowsi University of Mashhad, Mashhad 9177948974, Iran

[+] These authors contribute equally to this work.

* Authors to whom correspondence should be addressed.

Prof. Jong Seung Kim, E-mail: jongskim@korea.ac.kr

Prof. Xiaogang Liu, E-mail: xiaogang_liu@sutd.edu.sg

Prof. Mingle Li, E-mail: limingle@szu.edu.cn

Dr. Yunjie Xu, E-mail: xuyunjie87@korea.ac.k

This file includes

1. Materials and Instruments

1.1. Materials

Materials and Instruments for Chemical Synthesis and Characterization

β-Nicotinamide adenine dinucleotide reduced disodium salt hydrate (NADH, CAS No. 606-68-8) was purchased from Sigma Aldrich. 5-Bromobenzothiophene (98%, CAS No. 4923-87-9) and sodium *tert*-butoxide (97%, CAS No. 865-48-5), tris(dibenzylideneacetone)dipalladium, (97%, CAS No. 51364-51-3), anhydrous toluene (99.8%, CAS No. 108-88-3, packaged under Argon), *N*-iodosuccinimide (97%, CAS No. 516-12-1), 1,3-dibenzofuran (97%, CAS No. 5471-63-6), trimethyl borate, (99%, CAS No. 121-43-7), and 2,3-dichloro-5,6-dicyano-1,4-benzoquinone(CAS No. 84-58-2) were purchased from Alfa Aesar. 2,4-Dimethylpyrrole (CAS No. 625-82-1) was purchased from carbosynth. 2-Bromothiophene (98%, CAS No. 1003-09-4), 4-bromotriphenylamine (97%, CAS No. 35809-26-4), potassium carbonate (CAS No. 584-08-7), and trifluoroacetic acid (CAS No. 76-05-1) were purchased from TCI (Tokyo Chemical Industry). Tetrakis(triphenylphosphine)palladium(0) (CAS No. 14221-01-3) was purchased from SY Innovation. The calcein-AM/PI Double Stain Kit was obtained from Invitrogen. The cellular NAD/NADH assay kit (colorimetric) was purchased from Promega (catalog nos. G9071). The FITC annexin V detection kit was purchased from BD PharmingenTM (Cat No. 556547). The nuclear imaging agent Hoechst 33342 was purchased from Invitrogen (Cat No. H3570). 9,10- anthracenediyl-bis(methylene) dimalonic acid (CAS No. 307554-62-7), the superoxide assay kit (dihydrorhodamine 123, DHR123) for superoxide radical ($O_2^{-\bullet}$) detection, 2'-7'dichlorofluorescin diacetate (DCFH-DA) were purchased from Sigma-Aldrich. The singlet oxygen trapping agent 2,2,6,6-tetramethyl-4-piperidine (TEMP) and the free radicals trapping agent 5,5-dimethyl-1-pyrroline *N*-oxide (DMPO) were purchased commercially from TCI.

1.2. Instruments

Fluorescence and UV-vis absorption spectra were recorded using a Shimadzu RF-5301PC fluorometer and an Agilent 8453 spectrophotometer, respectively. ^{1}H and ^{13}C NMR spectra were collected on a Bruker 500 MHz spectrometer. Confocal laser scanning microscope (CLSM) images were obtained using an Olympus FV3000 confocal laser scanning microscope. The absorbance measurements for cell studies were determined using a SpectraMax Gemini EM microplate reader (Molecular Devices, San Jose, CA, USA). Electron spin resonance (EPR) experiments were performed on an ESR Spectrometer (JEOL, JEX-X320).

2. Synthesis of thiophene-bridged heavy-atom-free BODIPY photosensitizers (PSs)

2.1. Overall synthetic schemes

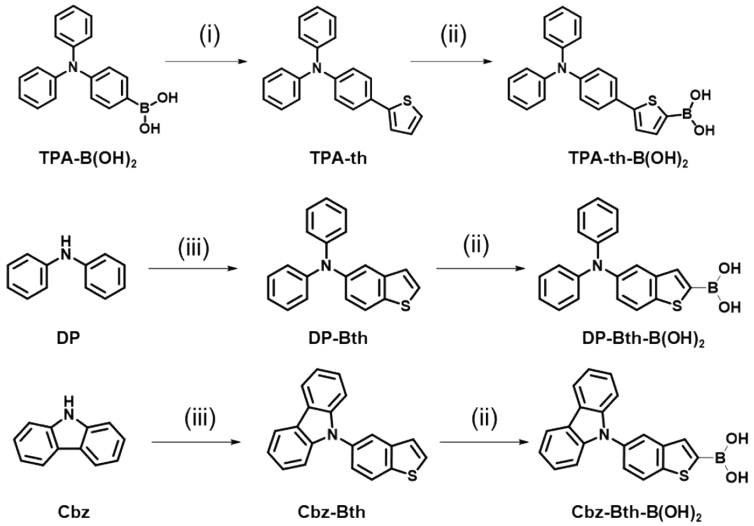

Scheme S1. Synthesis of thiophene-conjugated donors (TPA-th, DP-Bth, and Cbz-Bth). Reagents and conditions: (i) 2-Bromothiophene, Potassium carbonate, Tetrakis(triphenylphosphine)palladium(0), THF, reflux 3 h; (ii) Butyllithium, Trimethyl borate, Hydrochloric acid. Tetrahydrofuran, -78 °C; iii) 5-bromo-benzothiophene, sodium tert-butoxide, Tris(dibenzylideneacetone)dipalladium, toluene, reflux, 2 h.

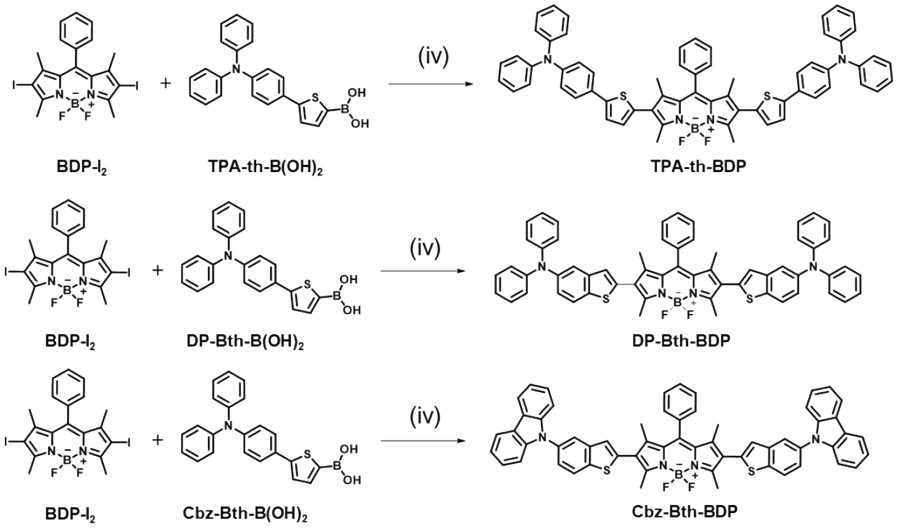

Scheme S2. Synthesis of thiophene-bridged BODIPY PSs (**TPA-th-BDP**, **DP-Bth-BDP**, and **Cbz-Bth-BDP**). Reagents and conditions: (iv) Potassium carbonate, Tetrakis(triphenylphosphine)palladium(0). Toluene, Ethanol, Water (v/v/v = 2:2:1), reflux 3 h.

2.2. Detailed synthetic procedures

2.2.1. Synthesis of donor-thiophene units (TPA-th, DP-Bth, and Cbz-Bth)

TPA-$B(OH)_2$ was synthesized from the previously reported method.[1]

TPA-th-$B(OH)_2$ was synthesized from the previously reported method. [2]

DP-Bth was synthesized from the previously reported method. [3]

Cbz-Bth was synthesized from the previously reported method. [3]

DP-Bth-$B(OH)_2$

A solution of DP-Bth (1 g, 3.32 mmol) in anhydrous THF (20 mL) was cooled to -78 °C under an argon atmosphere. Then, *n*-butyllithium (2.5 M in hexane, 3.65 mmol) was then slowly added dropwise to the mixture. The reaction mixture was stirred for one hour at -78 °C. After stirring, trimethyl borate (0.43 mL, 3.98 mmol) was added to the mixture at once, and the mixture was allowed to warm to room temperature overnight. Then the reaction was quenched with 1 *N* aqueous hydrochloride acid solution, and dichloromethane was used to extract the mixture. The organic layer was washed with brine, combined and dried over magnesium sulfate. The solvent was removed, and the residue was recrystallized using a small amounts of dichloromethane, followed by the addition of hexane to yield white-yellowish powder (82% of yield). ^{1}H NMR (500 MHz, DMSO) δ 8.48 (s, 1H), 7.90 (d, J = 8.7 Hz, 1H), 7.80 (s, 1H), 7.52 (d, J = 2.0 Hz, 1H), 7.31 – 7.26 (m, 4H), 7.10 – 7.08 (m, 1H), 7.03 – 6.98 (m, 6H).^{13}C NMR (126 MHz, DMSO) δ 148.10, 144.48, 142.29, 138.67, 132.90, 129.94, 123.99, 123.93, 123.71, 123.57, 122.96, 120.08. LC-MS calcd for $C_{20}H_{16}BNO_2S$ (M), $[M+H]^+$ = 345.1, found 346.1

Cbz-Bth-$B(OH)_2$

A solution of Cbz-Bth (1 g, 3.34 mmol) in anhydrous THF (20 mL) was cooled to -78 °C under an argon atmosphere. Then, n-butyllithium (2.5 M in hexane, 3.67 mmol) was slowly added dropwise to the mixture. The reaction mixture was stirred for one hour at -78 °C. After stirring, trimethyl borate (0.43 mL, 4.01 mmol) was added to the mixture in a single portion, and the reaction was allowed to warm to room temperature overnight. Then the reaction was quenched with 1 N aqueous hydrochloric solution, and the mixture was extracted with dichloromethane. The organic layer was washed with brine, combined, and dried over magnesium sulfate. After solvent removal, the residue was recrystallized using a small amount of dichloromethane, followed by the addition of hexane, to yield a white-yellowish powder (77% of yield). ^{1}H NMR (500 MHz, DMSO) δ 8.27 (m, 3H), 8.16 (d, J = 1.9 Hz, 1H), 7.96 (d, J = 5.4 Hz, 1H), 7.58 (m, 2H), 7.43 (ddd, J = 18.0, 12.5, 4.5 Hz, 4H), 7.30 (m, 2H).^{13}C NMR (126 MHz, DMSO) δ 142.31, 142.26, 141.08, 133.72, 133.31, 126.73, 124.61, 124.30, 123.11, 122.70, 120.99, 120.43, 110.13. $C_{20}H_{14}BNO_2S$, $[M+H]^+$ = 343.1, found 344.1

2.2.2. Synthesis of thiophene-bridged BODIPY PSs

Synthesis of BDP-I_2

BDP-I_2 was synthesized from the previously reported method.[4]

Synthesis of TPA-BDP

TPA-BDP was synthesized from the previously reported method.[5]

Synthesis of TPA-th-BDP

TPA-th-BDP was synthesized using the Suzuki coupling reaction. A solution of BDP-I_2 (300 mg, 0.52 mmol), compound **1** (452 mg, 1.56 mmol), tetrakis(triphenylphosphine)palladium(0) (23 mg, 0.02 mmol), and potassium carbonate (715 mg, 5.2 mmol) in 50 mL of a degassed toluene/ethanol/water mixture (2:2:1 v/v/v) was heated to reflux for 24 h under nitrogen. After cooling to room temperature for 3 h, the toluene layer was separated from the aqueous layer. The organic layer was washed successively with dichloromethane and dried over anhydrous magnesium sulfate. Then, the solvent was evaporated under reduced pressure. The residue was purified by silica-gel column chromatography (DCM: Hex = 1: 1). Finally, TPA-th-BDP was obtained as a Blue-violet solid in a 47.5% yield.

Synthesis of DP-Bth-BDP

DP-Bth-BDP was synthesized using the Suzuki coupling reaction. A solution of BDP-I_2 (300 mg, 0.52 mmol), compound 5 (539 mg, 1.56 mmol), tetrakis(triphenylphosphine)palladium(0) (23 mg, 0.02 mmol), and potassium carbonate (715 mg, 5.2 mmol) in 50 mL of a degassed toluene/ethanol/water mixture (2:2:1 v/v/v) was heated to reflux for 24 h under nitrogen. The reaction mixture was cooled to room temperature for 3 h, and the toluene layer was separated from the aqueous layer. The organic layer was washed successively with dichloromethane and dried over anhydrous magnesium sulfate. Then, the solvent was evaporated under reduced pressure. The crude was purified by silica-gel column chromatography (DCM: Hex = 1: 1). Finally, DP-Bth-BDP was obtained as a deep-violet solid in a 47.5% yield. ^{1}H NMR (500 MHz, $CDCl_3$) δ 7.68 (d, J = 8.7 Hz, 5H), 7.51 (s, 2H), 7.47 (d, J = 2.1 Hz, 2H), 7.38 (d, J = 1.2 Hz, 6H), 7.24 (dd, J = 8.5, 7.4 Hz, 9H), 7.15 – 7.14 (m, 1H), 7.13 – 7.12 (m, 1H), 7.10 (dd, J = 8.6, 1.1 Hz, 8H), 7.01 (d, J = 7.3 Hz, 4H), 6.90 (s,2H), 2.65 (s, 6H), 1.43 (s, 6H). ^{13}C NMR (126 MHz, $CDCl_3$) δ 206.94, 147.98, 145.05, 141.19, 135.97, 135.39, 135.22, 135.17, 129.33, 129.22, 127.90, 127.65, 124.35, 123.94, 122.67, 122.59, 119.08, 77.27, 77.02, 76.76, 53.40, 31.03, 13.03. LC-MS calcd for $C_{59}H_{45}BF_2N_4S_2$, $[M+H]^+$ = 922.31, found 922.84.

Synthesis of Cbz-Bth-BDP

Cbz-Bth-BDP was synthesized using the Suzuki coupling reaction. A solution of BDP-I_2 (300 mg, 0.52 mmol), compound 7 (535 mg, 1.56 mmol), tetrakis(triphenylphosphine)palladium(0) (23 mg, 0.02 mmol), and potassium carbonate (715 mg, 5.2 mmol) in 50 mL of a degassed toluene/ethanol/water

mixture (2:2:1 v/v/v) was heated to reflux for 24 h under nitrogen. After the reaction, the mixture was allowed to cool to room temperature over 3 h, and the toluene layer was separated from the aqueous layer. The organic layer was then washed successively with dichloromethane and dried over anhydrous magnesium sulfate. The solvent was evaporated under reduced pressure, and the residue was purified by silica-gel column chromatography (DCM: Hex = 1: 1) mixture as the eluent. Finally, Cbz-Bth-BDP was obtained as a magenta solid in 37% yield. ^{1}H NMR (500 MHz, CD_2Cl_2) δ 8.11 – 8.07 (m, 4H), 7.99 – 7.97 (m, 2H), 7.91 – 7.89 (m, 2H), 7.45 – 7.42 (m, 3H), 7.37 – 7.32 (m, 12H), 7.23 – 7.19 (m, 4H), 7.14 – 7.13 (m, 2H), 2.62 (s, 6H), 1.18 (s, 6H). ^{13}C NMR (126 MHz, CD_2Cl_2) δ 147.90, 141.24, 132.98, 129.52, 125.95, 124.61, 123.38, 123.23, 122.22, 121.98, 121.91, 121.67, 121.25, 120.22, 119.87, 109.82, 53.88, 53.66, 53.44, 53.23, 53.01, 30.54, 13.66, 12.54. LC-MS calcd for $C_{59}H_{41}BF_2N_4S_2$ $[M-H]^+$, 917.2834; found, 917.20.

[1]H NMR, [13]C NMR, and HRMS

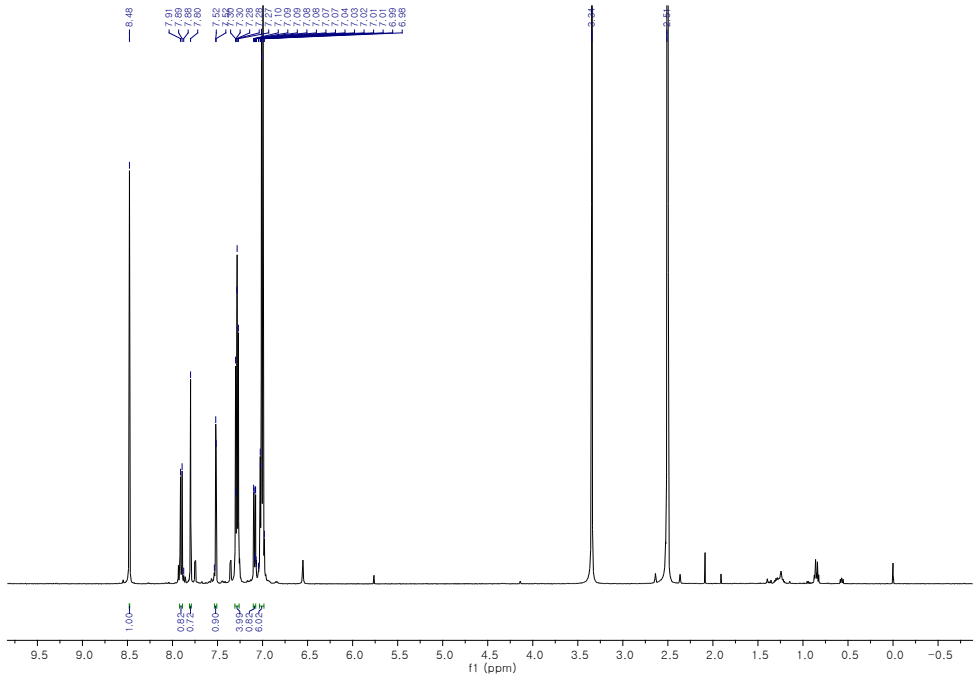

Figure S1. [1]H NMR spectrum (500 MHz) of **DP-Bth-B(OH)$_2$** in DMSO-d$_6$.

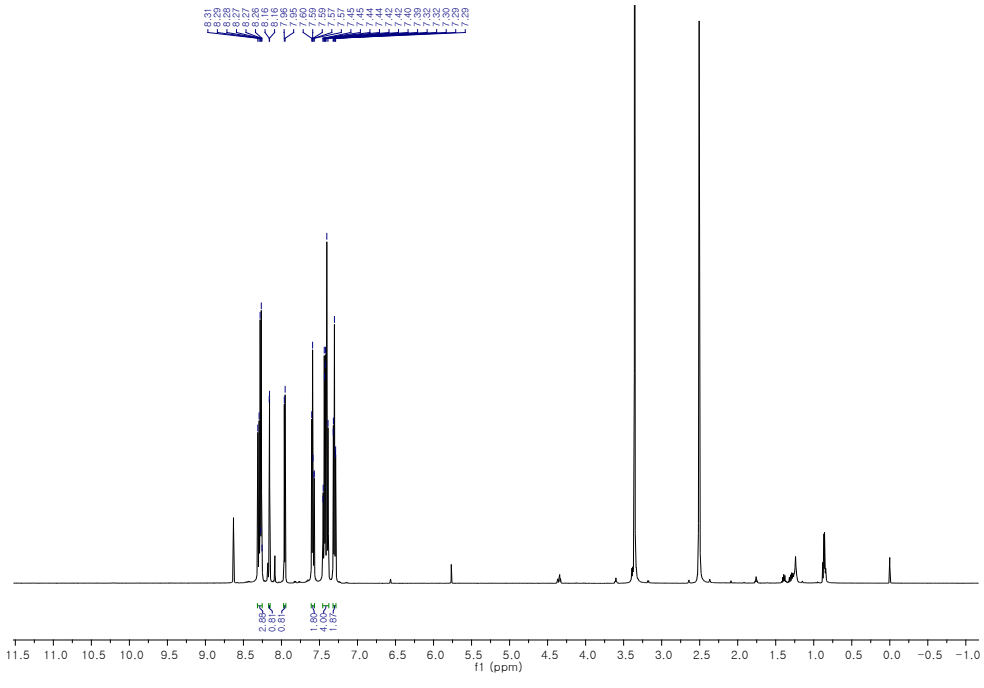

Figure S2. [1]H NMR spectrum (500 MHz) of **Cbz-Bth-B(OH)$_2$** in DMSO-d$_6$.

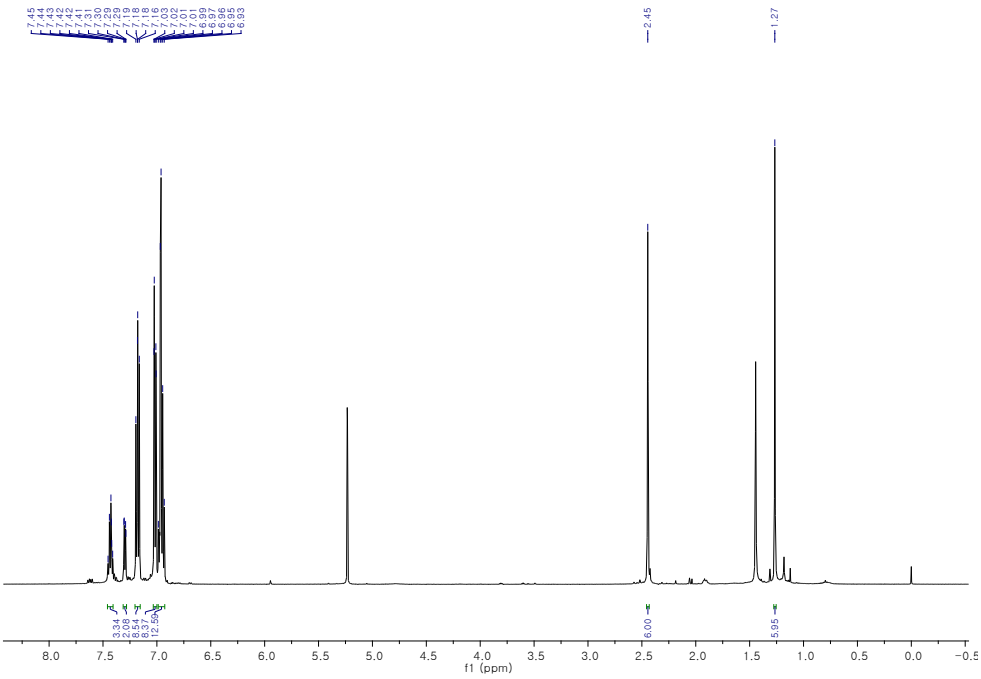

163

164 **Figure S3.** ^{1}H NMR spectrum (500 MHz) of **TPA-BDP** in CD_2Cl_2.

165

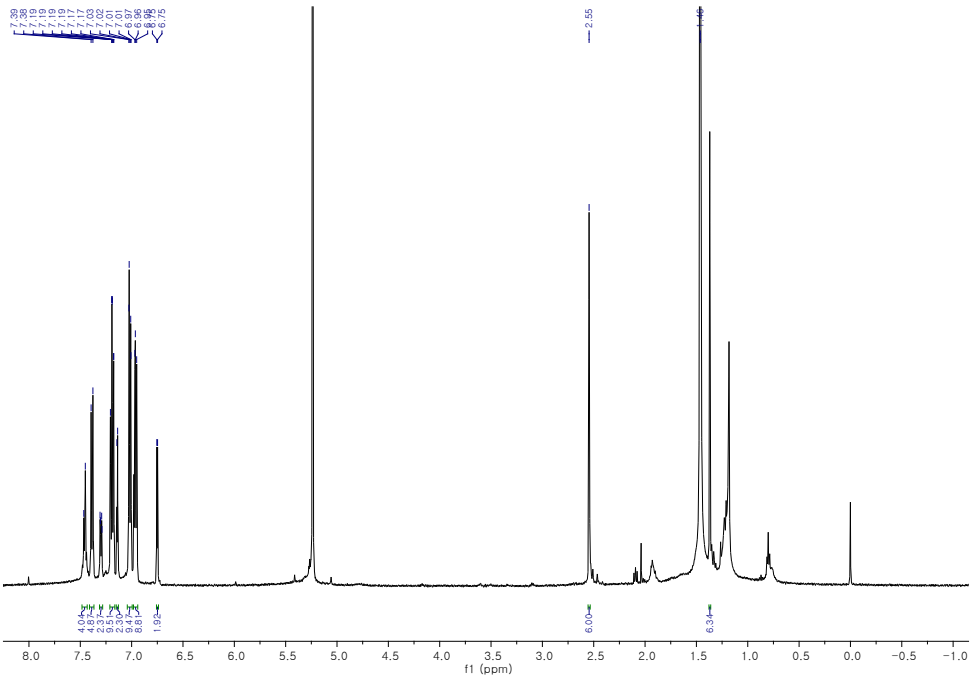

166

167 **Figure S4.** ^{1}H NMR spectrum (500 MHz) of **TPA-th-BDP** in CD_2Cl_2.

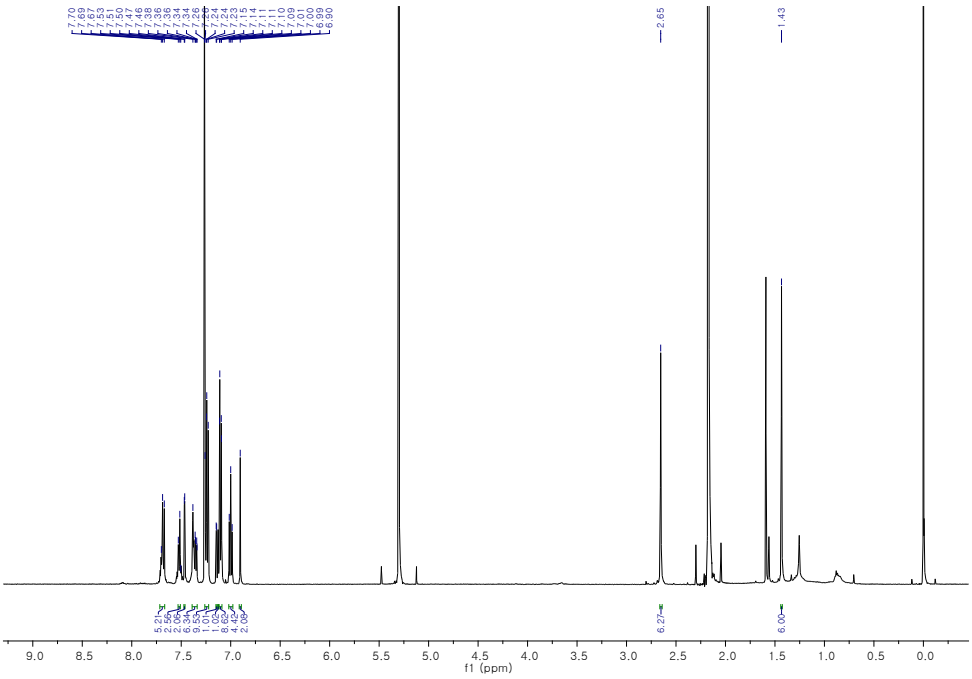

168

169 **Figure S5.** ^{1}H NMR spectrum (500 MHz) of **DP-Bth-BDP** in CD_2Cl_2.

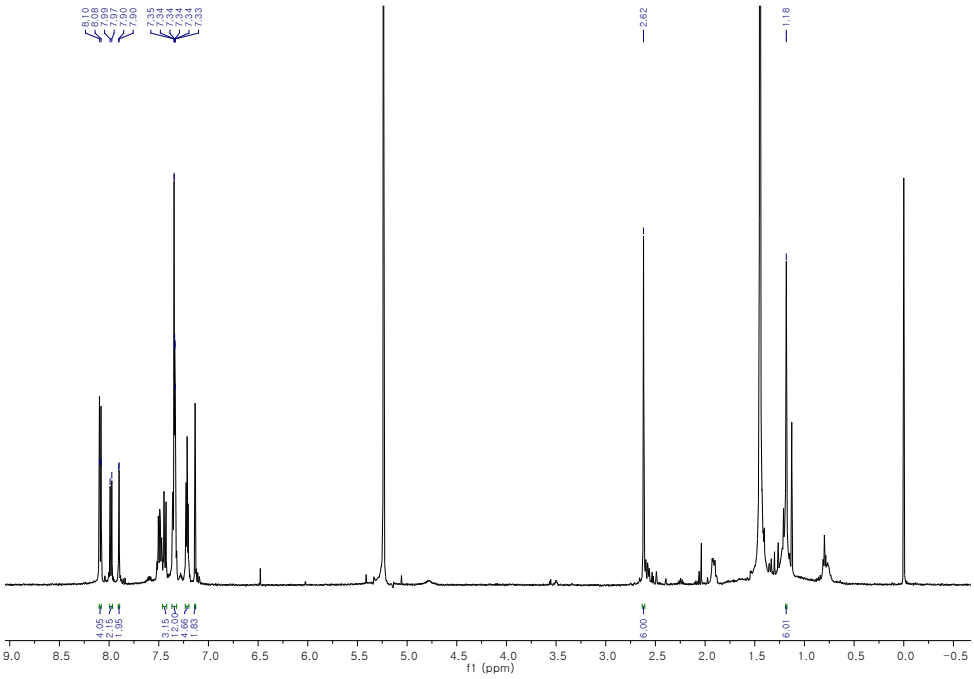

170

171 **Figure S6.** ^{1}H NMR spectrum (500 MHz) of **Cbz-Bth-BDP** in CD_2Cl_2.

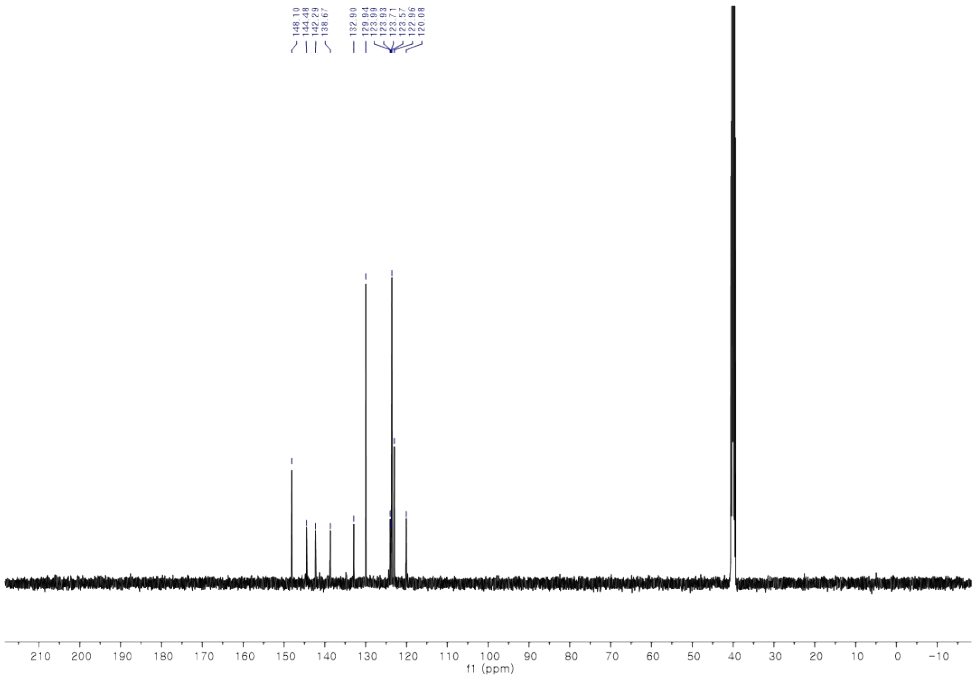

172

173 **Figure S7.** ^{13}C NMR spectrum (500 MHz) of **Cbz-Bth-B(OH)$_2$** in DMSO-d$_6$.

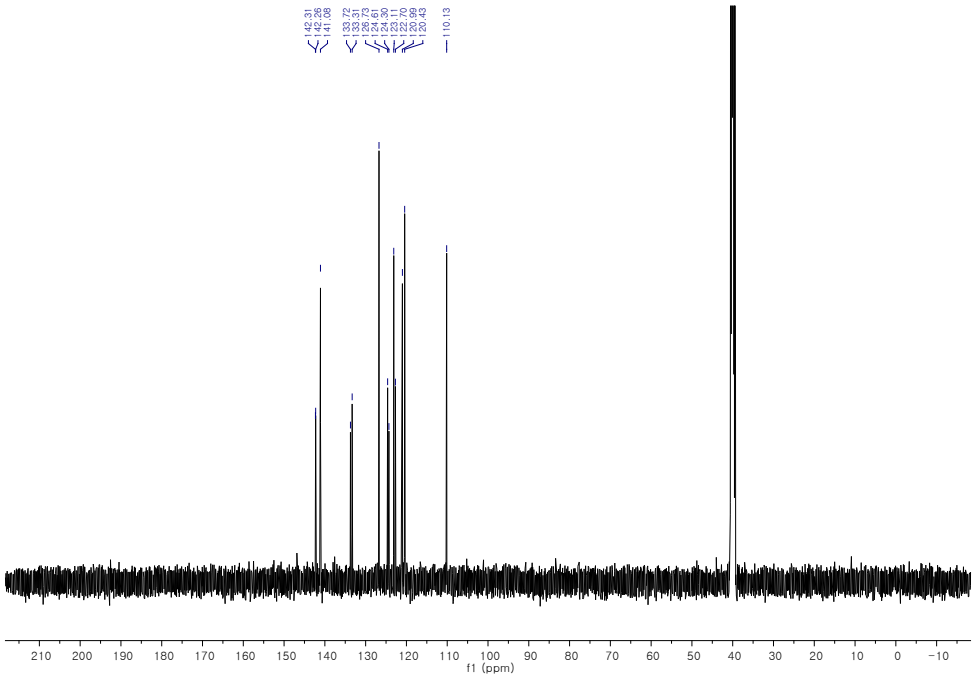

174

175 **Figure S8.** ^{13}C NMR spectrum (500 MHz) of **Cbz-Bth-BDP** in DMSO-d$_6$.

176

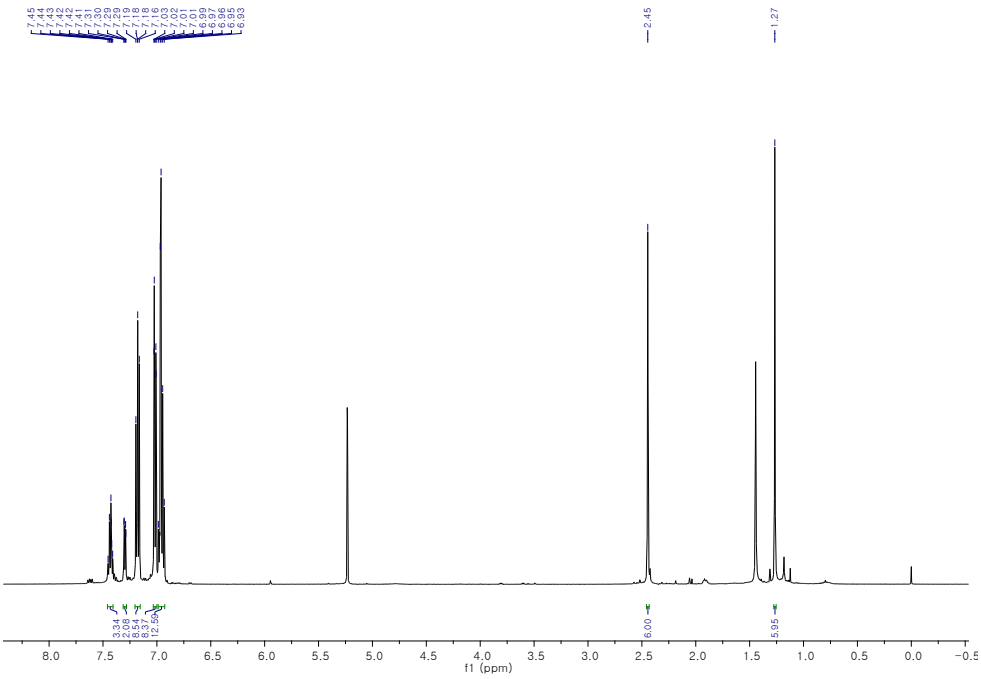

177

178 **Figure S9.** ^{13}C NMR spectrum (500 MHz) of **TPA-BDP** in CD_2Cl_2.

179

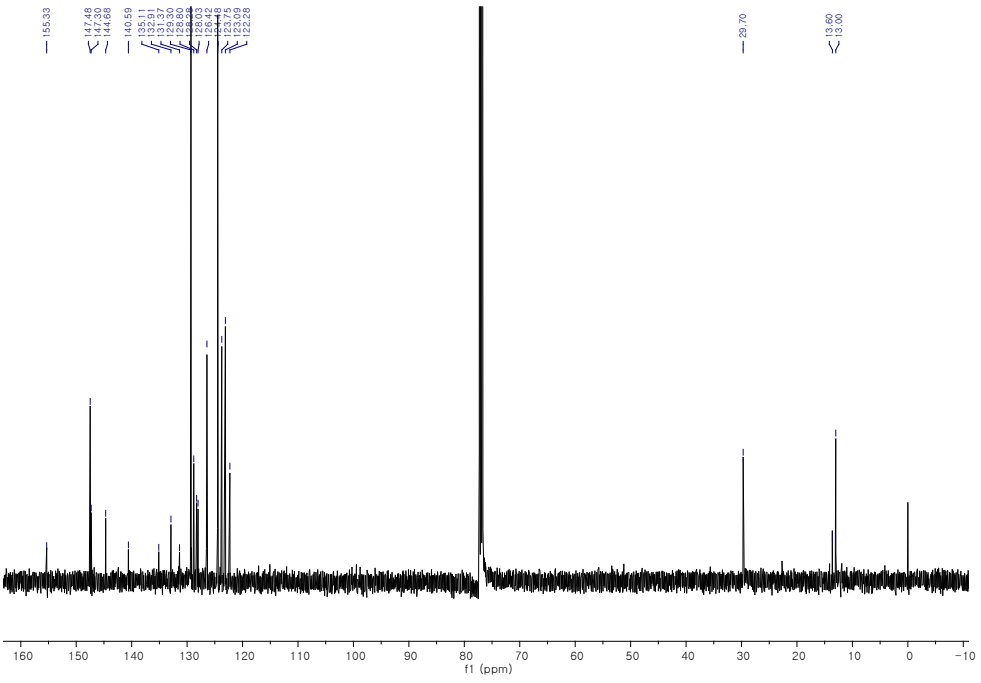

180

181 **Figure S10.** ^{13}C NMR spectrum (500 MHz) of **TPA-th-BDP** in CD_2Cl_2.

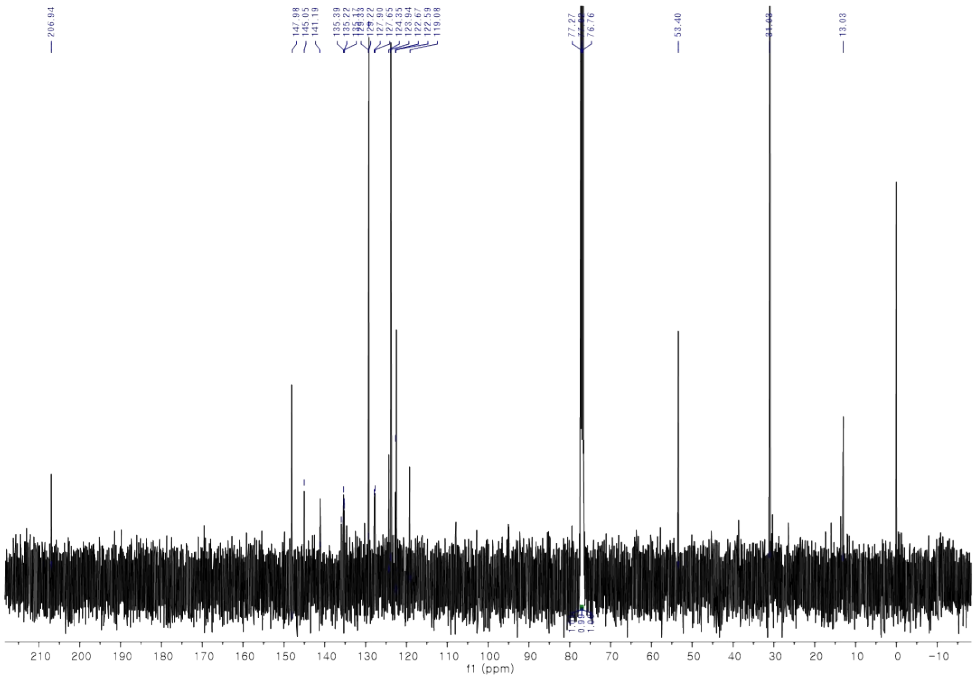

182

183 **Figure S11.** ^{13}C NMR spectrum (500 MHz) of **DP-Bth-BDP** in CD_2Cl_2.

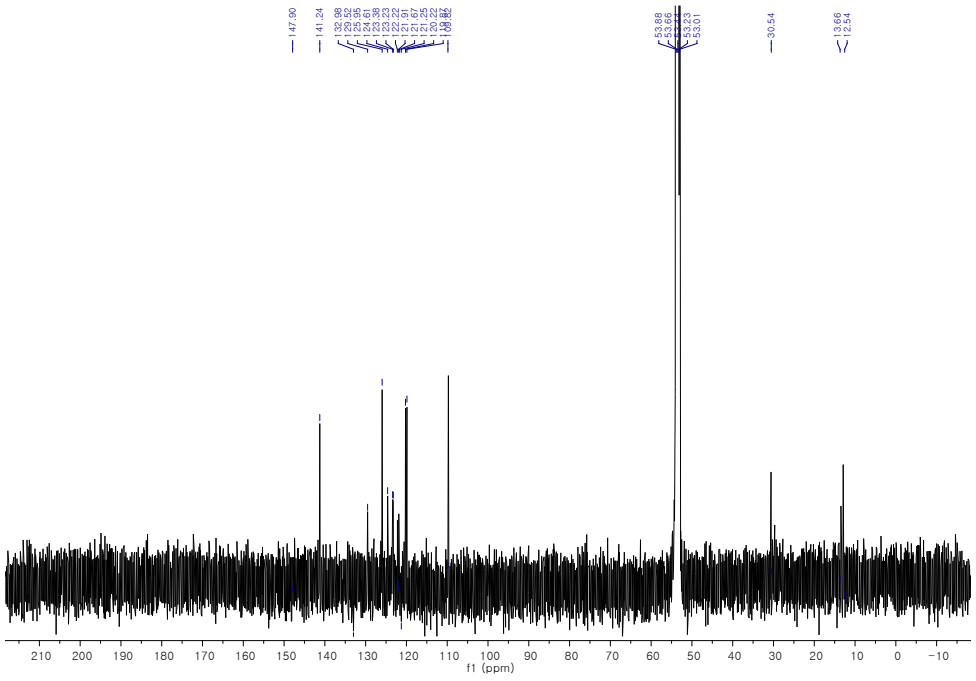

184

185 **Figure S12.** ^{13}C NMR spectrum (500 MHz) of **Cbz-Bth-BDP** in CD_2Cl_2.

186

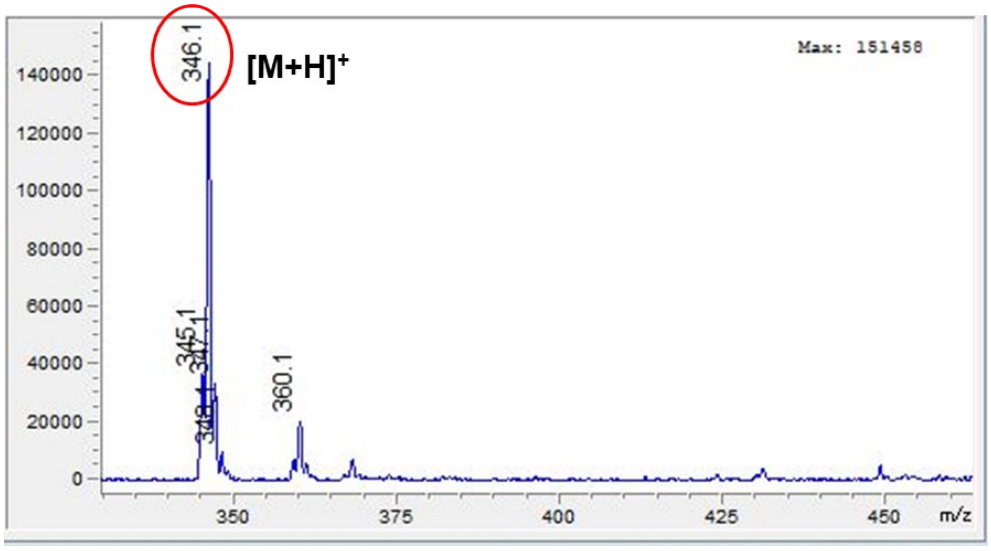

187

188 **Figure S13.** HRMS (ESI) of **DP-Bth-B(OH)$_2$**.

189

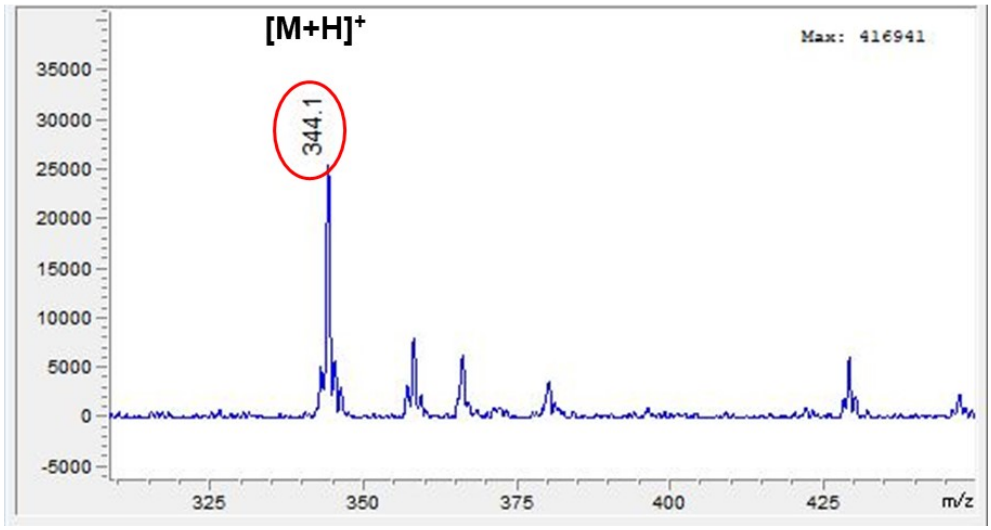

190

191 **Figure S14.** HRMS (ESI) of **Cbz-Bth-B(OH)$_2$**.

192

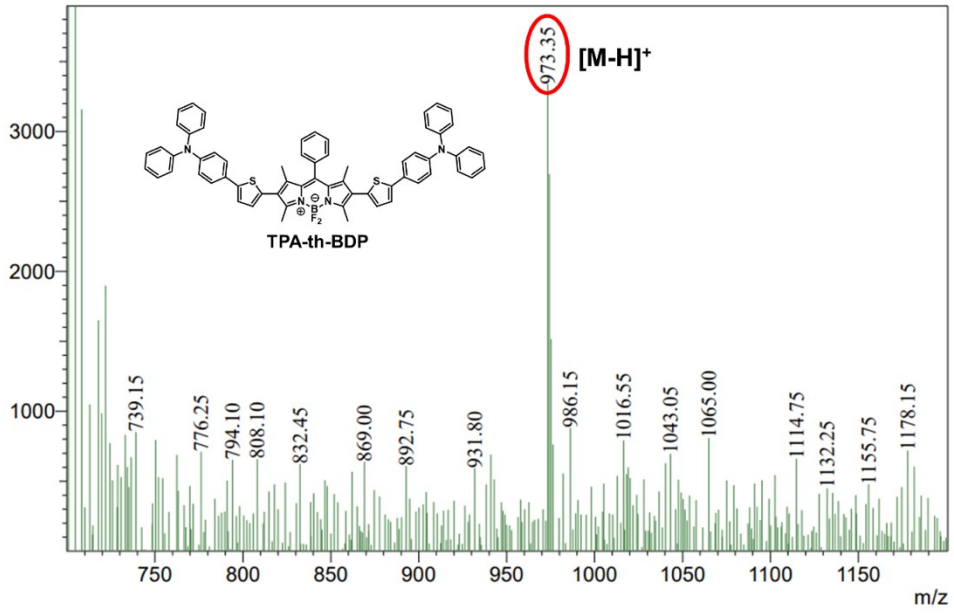

193

194 **Figure S15.** HRMS (ESI) of **TPA-th-BDP.**

195

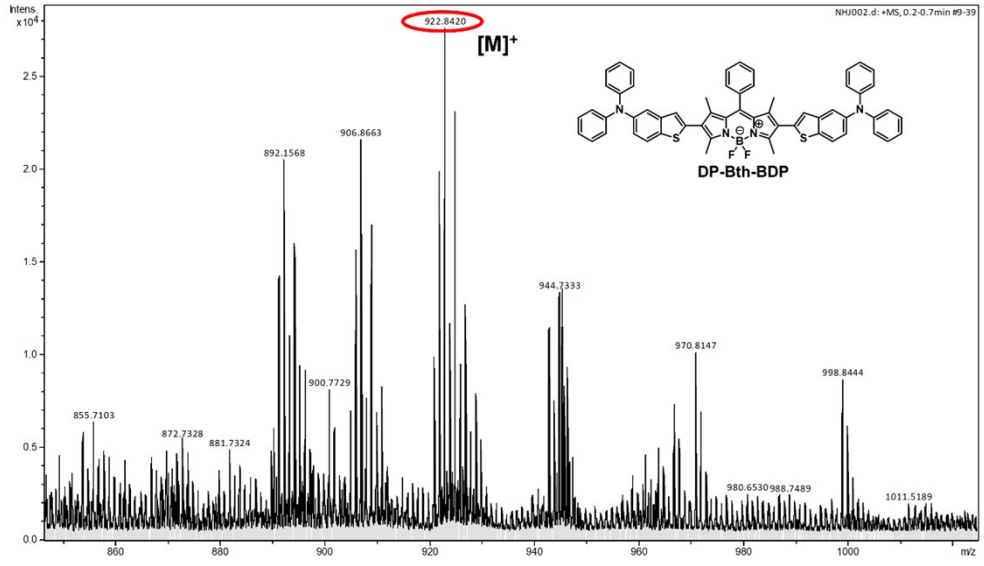

196

197 **Figure S16.** HRMS (ESI) of **DP-Bth-BDP**.

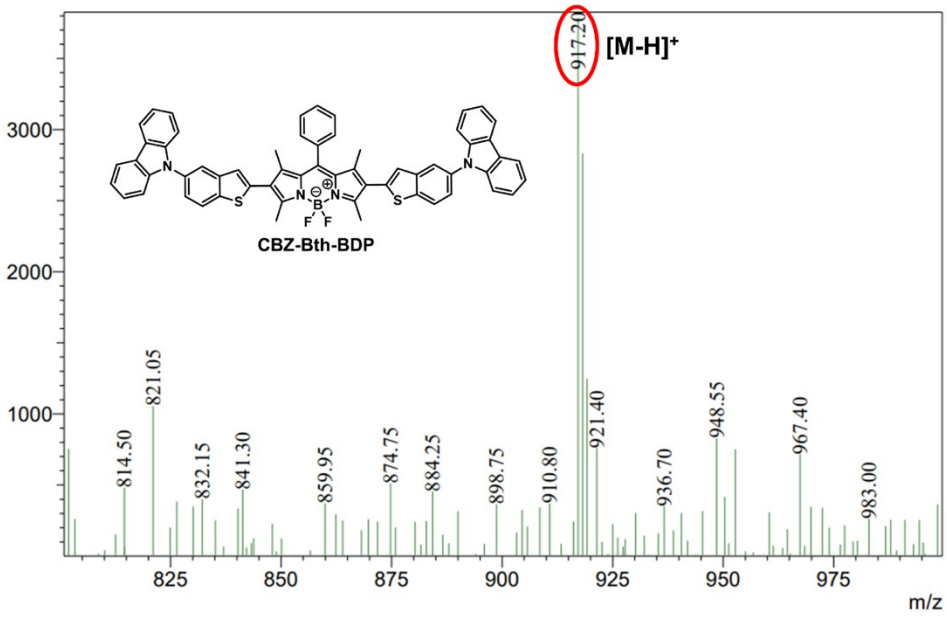

198

199 **Figure S17.** HRMS (ESI) of **Cbz-Bth-BDP**.

200

201

3. Additional experimental details and methods

Fluorescence Quantum Yield Measurements

Rhodamine 6G (Φs = 0.93 in methanol) was used as the reference to determine the relative fluorescence quantum yields of the synthesized compounds.[6]

$$\Phi_x = \Phi_s(F_x/F_s)(A_s/A_x)(\lambda_{exs}/\lambda_{exx})(n_x/n_s)$$

where Φ represents the quantum yield; F is the integrated area under the corrected emission spectrum; A stands for the absorbance at the excitation wavelength; λ_{ex} is the excitation wavelength; and the subscripts x and s refer to the unknown compound and the reference, respectively. The refractive index of the solvent is denoted by n. Due to the low concentrations of the solutions (10^{-6}-10^{-7} mol/L), changes in the refractive index were considered negligible. All values for relative polarity were normalized from measurements of solvent shifts in absorption spectra, with data extracted from Christian Reichardt, Solvents and Solvent Effects in Organic Chemistry, Wiley-VCH Publishers, 3rd ed., 2003.

ROS detection

1) DCFH Assay

General ROS generation was measured using 2,7-dichlorodihydrofluorescein (DCFH). Since DCFH tends to self-oxidize upon prolonged storage, a more stable derivative, DCFH-DA, was acquired commercially and hydrolyzed to prepare DCFH stock solutions. The protocol was as follows: 0.5 mL of 1 mM DCFH-DA in ethanol stock solution was mixed with 2 mL of 10 mM NaOH aqueous solution and stirred in the dark for 30 min to prepare the DCFH stock solution. When DCFH reacts with reactive oxygen species, green fluorescence (λ_{em} = 523 nm) is generated. To compare ROS generation, the synthesized photosensitizers were irradiated with a 530 nm PDT lamp, and the fluorescence intensity of DCFH was recorded at 523 nm.

2) DHR123 Assay

DHR123 (Dihydrorhodamine 123) was used as the superoxide radical indicator in solution tests. This indicator is converted to Rhodamine 123 in the presence of $O_2^{-\bullet}$. Solutions of thiophene-bridged BODIPY PSs (**Cbz-Bth-BDP**, **DP-Bth-BDP**, and **TPA-th-BDP)** were prepared at a concentration of 5 μM, and DHR123 was prepared at a concentration of 10 μM in PBS 0.01 M (pH = 7.4) in 10% DMSO. The cuvettes containing the test substances were exposed to a green PDT Lamp (power density: 10 mW cm^{-2}) for varying durations (0, 10, 20, 30…80, 90, and 100 seconds). The fluorescence spectra were recorded immediately following each irradiation period.

3) HPF Assay

HPF (Hydroxylphenyl Fluorescein) was utilized as a chemical sensor specifically for hydroxyl radicals

among type I ROS. HPF is specifically oxidized by $OH^{\cdot}$ and converted to strongly fluorescent fluorescein at 519.5 nm wavelength. The fluorescence intensity of HPF (10 μM) was measured upon irradiation at 530 nm with a PDT Lamp (light power intensity: 100 mW cm^{-2}, 10 s interval). Each photosensitizer's concentration was 5 μM in PBS (10 mM, pH 7.4, containing 10% DMF). Since DMSO can scavenge $OH^{\cdot}$, the HPF stock solution was prepared in DMF solvent. The fluorescence intensity ratio (F/F_0) of HPF at 519.5 nm was recorded (F_0: each compound's fluorescence intensity of HPF without irradiation).

4) ABDA Assay

Singlet oxygen generation by thiophene-bridged BODIPY PSs **(Cbz-Bth-BDP**, **DP-Bth-BDP**, and **TPA-th-BDP**) was tested using 9,10-anthracenedipropanoic acid (ABDA) as a singlet oxygen capture agent. In brief, the absorbance of ABDA at 378 nm was adjusted to approximately 1.0 in aqueous solution. Samples of BODIPY PSs (**Cbz-Bth-BDP**, **DP-Bth-BDP**, and **TPA-th-BDP)**, each at a concentration of 5 μM, were added to separate cuvettes. These cuvettes were then irradiated with a 530 nm PDT lamp (power density: 100 mW cm^{-2}) for various durations (0, 20, 40, 60…140, 160, and 180 seconds). The absorption spectra were recorded immediately after each irradiation period.

5) Singlet oxygen Quantum Yield

Calculations of relative singlet oxygen quantum yields were conducted based on previous literature. I_2-BDP (Φ_Δ = 0.85 in toluene) served as the standard for determining the relative singlet oxygen quantum yields of synthesized compounds.

A solution of 1,3-Diphenylisobenzofuran (DPBF, singlet oxygen trap) and the synthesized photosensitizers was added to a cuvette filled with air-saturated toluene. The solutions were kept in the dark until the absorbance readings stabilized, followed by continuous light irradiation. The absorption of DPBF at 414 nm was monitored every 3 seconds to obtain the decay rate of the photosensitizing processes. Measurements were performed using a green LED light source (10 mW cm^{-2}).

The $^1O_2$ quantum yields of the synthesized compounds were calculated using the equation.

$$\phi_\Delta(\mathrm{PS}) = \phi_\Delta(\mathrm{ref}) \times \frac{m(PS)}{m\,(ref)} \times \frac{F(ref)}{F\,(PS)} \times_{\mathrm{X}} \frac{m(PS)}{m\,(ref)}$$

where PS and ref represent the photosensitizer and the reference (I_2-BDP), respectively. *m* denotes the slope of the change in absorbance of DPBF at its absorbance maxima over irradiation time. *F* is defined as $F = 1\text{-}10^{-OD}$, where OD represents the optical density at the excitation wavelength. PF represents absorbed photonic flux (μEinstein $dm^{-3}s^{-1}$).

Electro Paramagnetic Resonance (EPR) Analysis

EPR spectrum was detected using 5,5-dimethyl-1-pyrroline *N*-oxide (DMPO) as a superoxide radical spin trapping agent, 5-tert-Butoxycarbonyl-5-methyl-1-pyrroline-N-oxide (BMPO) as a hydroxyl radical spin trapping agent, and 2,2,6,6-tetramethylpiperidine (TEMP) as a singlet oxygen spin trapping agent. The samples were prepared in 4 mL vials. All tests were conducted at 293 K with the following settings: Frequency = 9432.830 MHz; MOD Frequency = 100.00 kHz; Power = 3.0 mW.

1) Superoxide radical spin trapping experiment. Solutions of BODIPY PSs (TPA-BDP, **TPA-th-BDP**, **DP-Bth-BDP**, and **Cbz-Bth-BDP**) were prepared at a concentration of 200 μM in DMF. TEMP (50 μL mL^{-1}) was added to each solution in a 4 mL vial. The samples were irradiated using a 530 nm PDT lamp (power density: 100 mW cm^{-2}) for 3 min. EPR signals were measured immediately after photoirradiation.

2) For hydroxyl radical detection, BODIPY PSs (TPA-BDP, **TPA-th-BDP**, **DP-Bth-BDP**, and **Cbz-Bth-BDP**) were prepared at a concentration of 200 μM in THF. BMPO (50 μL mL^{-1}) was added to each solution in a 4 mL vial, followed by irradiation with a 530 nm PDT lamp (power density: 100 mW cm^{-2}) for 3 min. BMPO, $FeCl_2$, and H_2O_2 stocks were all prepared in deionized water (DW). PSs were prepared in THF. Standard Fenton reaction conditions were set up using $FeCl_2$ (1 mM, 1 eq) and H_2O_2 (10 mM, 1 eq) to validate hydroxyl radical generation.

3) For singlet oxygen detection, solutions of BODIPY PSs (TPA-BDP, **TPA-th-BDP**, **DP-Bth-BDP**, and **Cbz-Bth-BDP)** (200 μM in DMF), were prepared with the addition of DMPO (50 μL mL^{-1}) in 4 mL vials. The samples were exposed to a 530 nm PDT lamp (power density: 100 mW cm^{-2}) for 3 min.

Cyclic Voltammogram

Cyclic voltammetry was used to examine the electrochemical properties of the synthesized heavy-atom-free BODIPY PSs. Measurements were performed using a potentiostat (eDAQ, EA161) at a scan rate of 100 mV s^{-1}. Cyclic voltammetry data was obtained using ferrocene as a reference to measure the oxidation and reduction potentials of the synthesized heavy-atom-free BODIPY PSs (TPA-BDP, **TPA-th-BDP**, **DP-Bth-BDP**, and **Cbz-Bth-BDP**). Ferrocene was used as a reference in anhydrous dichloromethane with tetrabutylammonium hexafluorophosphate (0.1 M). The working electrode was prepared by drop-casting the sample onto a platinum (Pt) plate, while a Pt/Ti wire anode served as the counter electrode. A 3M NaCl solution was used as the reference electrode. Tetrabutylammonium hexafluorophosphate (NBu_4PF_6, 0.10 M) in distilled dichloromethane was used as the electrolyte solution. The energy gap between the highest occupied molecular orbital (HOMO) and lowest unoccupied molecular orbital (LOMO) levels was determined by measuring the onset oxidation potentials ($E_{OX\ onset}$). The LUMO and HOMO energy levels were determined using the following equations:

$$LUMO = - (4.8 + E_{Red} - E_{FC})\ (E_{FC}\text{: ferrocene's } E_{OX}^{onset})$$

$$HOMO = - (4.8 + E_{ox} - E_{FC})$$

UV optical band (band gap) = LUMO – HOMO

Computational Method

Quantum calculations for this study were performed using Gaussian 16. The Avogadro software was used to visualize molecular orbitals.[7] All calculations were performed at the M062X/def2-SVP level of theory with the SMD solvation model in a polar environment (water),[8] unless mentioned otherwise. The corrected linear solvation formalism was used to obtain the electronic energy of various excited states.

Given the limitations of the M062X functional in accurately describing the S_1(ET) state, the B3LYP/def2-SVP level of theory was utilized for the geometry optimization of the S_1(ET) state under the linear solvation formalism. To ensure complete charge separation during these calculations, two dihedral angles of the 6-position substituents were constrained to 90°. Following geometry optimization, the M062X/def2-SVP level of theory with the corrected linear solvation formalism was applied to calculate the electronic energy of the S_1(ET) state.

The ΔE_{ST} values were calculated based on the difference between the S_1 and T_n (n=1,2) energy levels. Spin-orbit coupling (SOC) values were calculated using ORCA 5.0 [9] based on the optimized S_1(ET) molecular structure, employing the M06-2X/def2-SVP level of theory alongside the linear solvation formalism.

The ionization potential (IP) and electron affinity (EA) of various substituents were calculated by first optimizing the geometries of the neutral molecules, followed by the corresponding radicals (cations for IP and anions for EA). The IP and EA values were then determined based on the Gibbs energy difference between the optimized radical and neutral species.

The electron affinity (EA) of the photosensitizers in the triplet state (T_1) was calculated through a multi-step process. First, the triplet state geometries were optimized using time-dependent density functional theory (TD-DFT). Subsequently, energy correction was applied using the corrected linear solvation formalism. Next, the corresponding anion was optimized. Finally, the EA values were determined based on the electronic energy difference between the optimized radical and neutral T_1 species.

Bio studies

1) Cell Culture

Human breast cancer cell lines MDA-MB-231, T47D, and MCF-7 were maintained in Roswell Park Memorial Institute (RPMI) 1640 medium (GIBCO), supplemented with 10% fetal bovine serum (HyClone), 100 U mL^{-1} penicillin, and 100 µg mL^{-1} streptomycin (HyClone). The cells were cultured in a humidified incubator (5% CO_2 at 37°C).

2) Cell Viability Assay

The cytotoxic effects of BODIPY PSs (TPA-BDP, **TPA-th-BDP**, **DP-Bth-BDP**, and **Cbz-Bth-BDP**) on MDA-MB-231 cells were determined using an Thiazolyl Blue tetrazolium bromide, 98% (MTT)-based cell viability assay kit. Briefly, ca. 8×10^3 MDA-MB-231 cells per well were seeded in a 96-well plate for 24 h at 37 ℃ in a humidified, 5% CO_2 atmosphere. The cells were then treated with different concentrations of Cbz-Bth-BDP (0, 0.5, 1, 2, 4, and 8 μM) to determine the IC_{50} value. 24 h later, the cells were subjected to photoirradiation (530 nm PDT Lamp, 10 min, 100 mW cm^{-2}). Following another day of incubation, 10 μL of MTT (5 mg mL^{-1}) was added to each well, and the cells were incubated for an additional 2–4 h. The medium was suctioned, and 150 μL of DMSO was added to dissolve the formazan crystals . Cell viability was determined using a multiplate reader (HOIL BIOMED Co.) by recording the absorbance at 570 nm. Cell viability was calculated using the following equation:

$$\text{Cell viability (\%)} = (\text{OD}_{ps} - \text{OD}_{blank\ control} / \text{OD}_{control} - \text{OD}_{blank\ control}) \times 100\%$$

3) Intracellular NADH Detection

The effect of BODIPY PSs (TPA-BDP, **TPA-th-BDP**, **DP-Bth-BDP**, and **Cbz-Bth-BDP**) on intracellular NADH levels was evaluated using the NAD^+/NADH-Glo™ Assay (bioluminescent) kit. In brief, MDA-MB-231 cells were seeded in a 96-well plate at a density of 1×10^4 per well and cultured in a cell incubator at 37 ℃. The cells were treated with the indicated drugs for 24 h, then the initial medium was discarded and replaced with 50 μL PBS. Following 530 nm photoirradiation for 10 min at a density of 100 mW cm^{-2}, the luminescence of the samples was measured according to the instructions of the manufacturer. The NAD^+/NADH ratios were calculated by dividing the luminescence of the NAD^+ samples by the luminescence of the NADH samples:

$$Ratio\ of\ NAD+/NADH = ((Luminescence\ of\ NAD\ samples))/(luminescence\ of\ NADH\ samples)$$

4) Western blot analysis

The expression of pyroptosis-associated proteins, including cleaved-caspase3, caspase3, and GSDME, was evaluated using western blot. After the treatment with BODIPY PSs (TPA-BDP, **TPA-th-BDP**, **DP-Bth-BDP**, and **Cbz-Bth-BDP**), the samples were harvested and washed with cold PBS. Cell lysates were prepared by incubating the cells in ice-cold radioimmunoprecipitation assay buffer, followed by sonication and centrifugation (20,000 g, 10 min). Protein concentrations were determined using a bicinchoninic acid (BCA) assay. 30-50 micrograms of total protein samples were separated by SDS-PAGE and transferred onto PVDF membranes. The membranes were blocked with 5% w/v skim milk and incubated overnight at 4 ˚C with primary antibody: GSDME (Abcam, catalog no. ab215191), cleaved-caspase3 antibody (Cell Signaling Technology, catalog no. 9661s), IL-1β (GeneTex, catalog no. GTX74034) and β-actin (Santa Cruz Biotechnology, catalog no. sc-47778) at a 1:1,000 dilution.

After washing with PBST, the membranes were incubated for 2 h with the relevant secondary antibody at a 1:1,000 dilution: anti-mouse (GeneTex, catalog no. GTX213110-01); anti-rabbit (Santa Cruz Biotechnology, catalog no. sc-2357). The protein expression levels were detected using enhanced chemiluminescence reagents (Luminate, Merck Millipore) and imaged using a Syngene Bio Imager (Synoptics Ltd., Cambridge, UK).

5) LDH Release Measurement

The release of LDH (lactose dehydrogenase) was measured using the CytoTox96™ Non-Radioactive Cytotoxicity Assay Kit (Promega, USA). For the positive control, maximum LDH release was induced by treating cells with a lysis buffer, followed by incubation at 37°C and 5% CO_2 for 45 min. The substrate solution, stored at -20°C, was warmed to room temperature before use. The substrate was added to the medium of each group and incubated in the dark for 30 min. A stop solution was then added to each well. The proportion of LDH released was calculated using the following formula: LDH Release (%) = (LDH treated average value - LDH untreated cells average value) / (LDH total lysis average value - LDH untreated cells average value) × 100. Absorbance was measured at 490 nm using a multi-plate reader (HOIL BIOMED Co.)

6) ATP Release Measurement

ATP release into the cell medium was determined to evaluate cell membrane damage. Cells were treated with the indicated drugs for 24 h, the medium was replaced with fresh medium, and the cells were exposed to photoirradiation (530 nm, 100 mW cm^{-2}, 10 min). After a further 6 h of incubation, the medium was collected and the ATP concentration was measured using a multi-plate reader.

7) 3D tumor spheroid inhibition

For 3D multicellular spheroids (MCSs), approximately 2×10^3 T47D cells per well were seeded in 96-well plates (U-shaped) (Sumitomo Bakelite, Japan). After 3 days of incubation, the T47D MCSs were treated with thiophene-bridged BODIPY PSs (**TPA-th-BDP**, **DP-Bth-BDP**, and **Cbz-Bth-BDP**) for 48 h and exposed to photoirradiation (530 nm, 100 mW cm^{-2}, 20 min). After culturing for another 48 h, the viability of the spheroid was determined using the CellTiter-Glo™ 3D Cell Viability Assay (Promega, Germany). The luminescence of ATP was detected through a multi-plate reader.

8) Live/Dead tumor spheroid Imaging

The anticancer effects of BODIPY PSs (TPA-BDP, **TPA-th-BDP**, **DP-Bth-BDP**, and **Cbz-Bth-BDP**) on tumor spheroids were determined using Calcein-AM/propidium iodide (PI) co-stain assay. In brief, after treatment with the indicated drugs, the spheroid samples were stained with Calcein-AM and PI in a cell incubator for 30 min. Following the washing with PBS, the stained spheroids were imaged using an Olympus FV3000 confocal laser scanning microscope.

9) Cell Morphology Imaging

Cellular photon-induced pyroptosis was detected by FITC-Annexin V/Hoechest 33342 staining. MDA-MB-231 cells were seeded in a 35 mm glass-bottom confocal dish and incubated for 24 h. The cells were treated with 2 μM of each BODIPY PSs (TPA-BDP, **TPA-th-BDP**, **DP-Bth-BDP,** and **Cbz-Bth-BDP**) and incubated for another 24 h. Morphological changes were visualized using fluorescence microscopy with excitation wavelengths of 405 nm and 640 nm. Emission was collected from 410 to 470 nm (blue channel) and 650 to 750 nm (red channel). For the Annexin V/Hoechest 33342 staining, 10X binding buffer was diluted into 1X binding buffer using distilled water. The working solution of 1 μg mL^{-1} of Hoechst 33342 was then prepared in 1X binding buffer. Cells were stained with a mixture of Hoechst 33342 and FITC-Annexin V after washing with binding buffer. Confocal images were captured using excitation of 405 and 488 nm, with emission signals collected at 430 to 470 nm (blue channel) and 500 to 540 nm (green channel).

10) Calcein/AM staining

To evaluate the effects of heavy-atom-free BODIPY PSs (**TPA-BDP**, **TPA-th-BDP**, **DP-Bth-BDP,** and **Cbz-Bth-BDP**) on MDA-MB-231 cells, ca. 3 ×10^4 MDA-MB-231 cells were seeded in glass bottom confocal dishes and cultured overnight. The cells were then incubated with 2 μM concentration of each BODIPY PSs (**TPA-BDP**, **TPA-th-BDP**, **DP-Bth-BDP,** and **Cbz-Bth-BDP**) for another 24 h. After exposure to 530 nm light (100 mW cm^{-2}) for 10 min, photo-irradiated cells were incubated for 24 h in the incubator (37 °C, 5% CO_2). They were then stained with 2 μM Calcein AM (Calcein acetoxymethyl ester, live cell marker, $\lambda ex =$ 473 nm and λem = 490-590 nm) and 4 μM PI (propidium iodide, dead cell marker, $\lambda ex =$ 559 nm and λem = 575-675 nm) for 30 min. After rinsing with PBS, cell imaging was carried out using an Olympus FV3000 confocal laser scanning microscope.

11) Statistical analyses

Data were analyzed by one-way analysis of variance using SPSS (version 21.0; IBM Corp., Armonk, NY, USA). Tukey's post hoc test was used to determine the significance of all pairwise comparisons of interest. Statistical significance was defined as $*P < 0.05$.

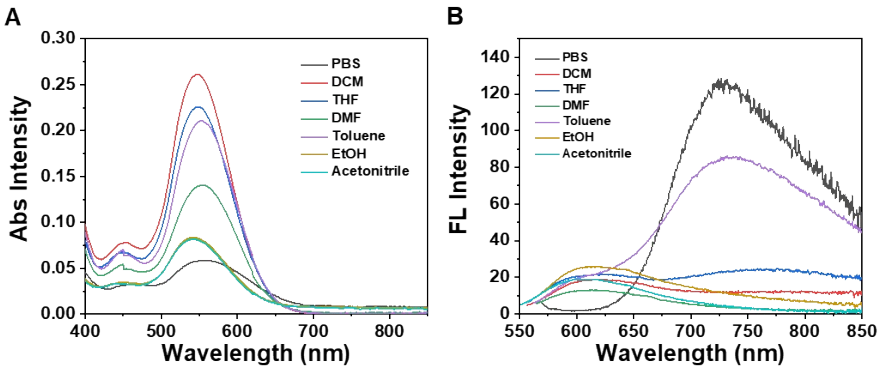

428

429 **Figure S18.** Photophysical properties of **TPA-th-BDP**. (A) Absorbance spectra and (B) Fluorescence
430 spectra of **TPA-th-BDP** in different organic solvents (PBS, DCM, THF, DMF, Toluene, EtOH, and
431 Acetonitrile). The concentration of **TPA-th-BDP** was maintained at 5 μM. Fluorescence spectra were
432 obtained upon excitation at the maximum excitation wavelength for each solvent.

433

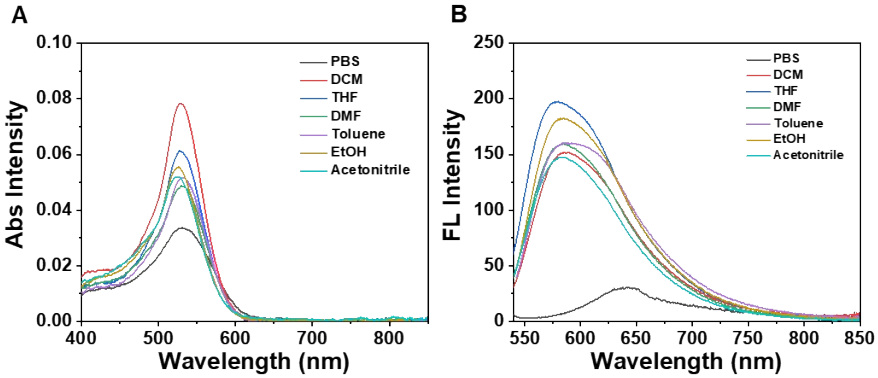

434

435 **Figure S19.** Photophysical properties of **DP-Bth-BDP**. (A) Absorbance spectra and (B) Fluorescence
436 spectra of **DP-Bth-BDP** in different organic solvents (PBS, DCM, THF, DMF, Toluene, EtOH, and
437 Acetonitrile). The concentration of **DP-Bth-BDP** was maintained at 5 μM. Fluorescence spectra were
438 obtained upon excitation at the maximum excitation wavelength for each solvent.

439

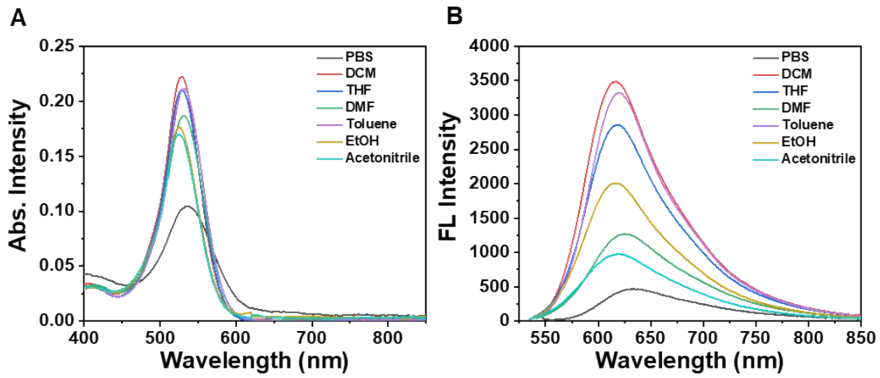

Figure S20. Photophysical properties of **Cbz-Bth-BDP**. (A) Absorbance spectra and (B) Fluorescence spectra of **Cbz-Bth-BDP** in different organic solvents (PBS, DCM, THF, DMF, Toluene, EtOH, and Acetonitrile). The concentration of **Cbz-Bth-BDP** was maintained at 5 μM. Fluorescence spectra were obtained upon excitation at the maximum excitation wavelength for each solvent.

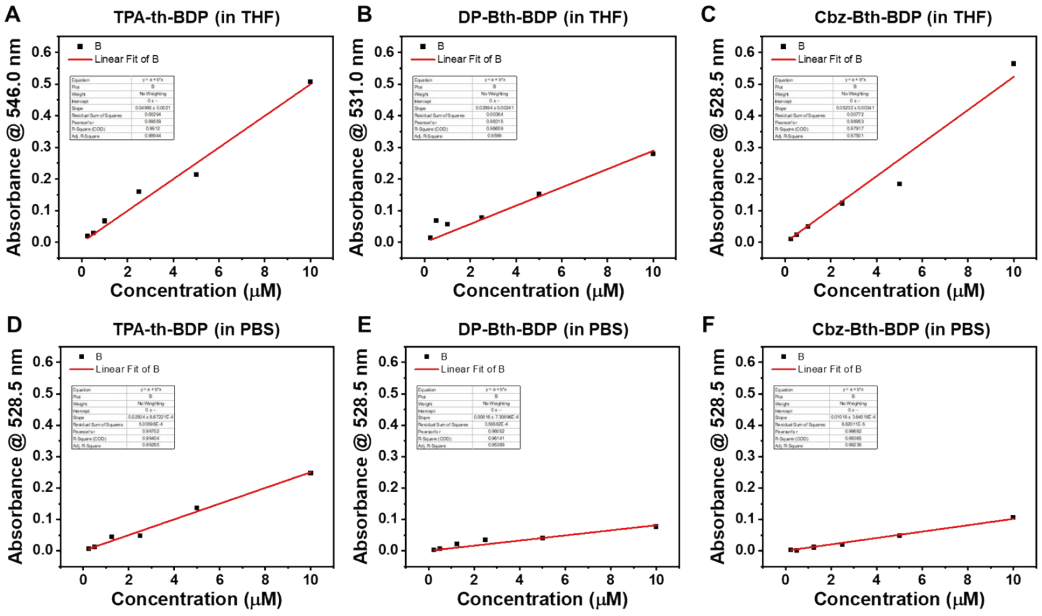

Figure S21. Determination of molar extinction coefficient (ε) for BODIPY PSs (**TPA-th-BDP**, **DP-Bth-BDP**, and **Cbz-Bth-BDP**) in THF (A-C) and PBS (D-F). UV-Vis absorption spectra of BODIPY derivatives were measured in THF and PBS at room temperature (25°C). The spectra were recorded at various concentrations ranging from 0.25 to 10 μM. Calibration curve of absorbance at the λ_{max} (nm) against the concentration of the compounds. The molar extinction coefficient (ε) was calculated from the slope of the linear regression, expressed as ε ($L \cdot mol^{-1} \cdot cm^{-1}$).

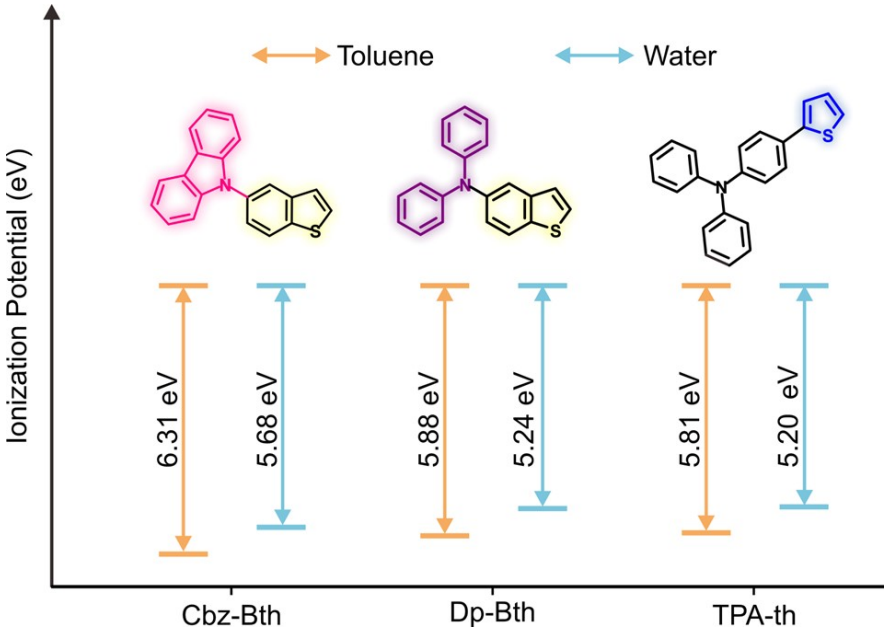

454

455 **Figure S22**. Ionization potential (IP) of various substituents in water and toluene. A lower IP value
456 indicates a stronger electron-donating ability.

457

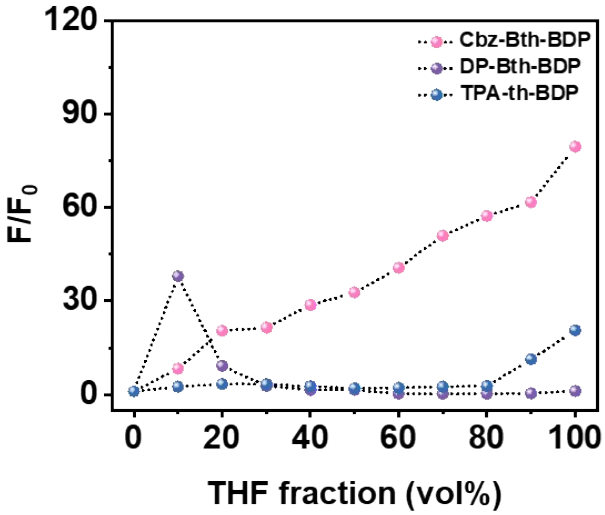

458

459 **Figure S23**. Fluorescence intensity of thiophene-bridged BODIPY PSs (**TPA-th-BDP**, **DP-Bth-BDP**,
460 and **Cbz-Bth-BDP**). The fluorescence intensity ratio (F/F_0) was measured in different fractions of THF
461 and H_2O. F and F_0 are the fluorescence intensities of BODIPY PCs in the absence and presence of
462 THF, respectively).

463

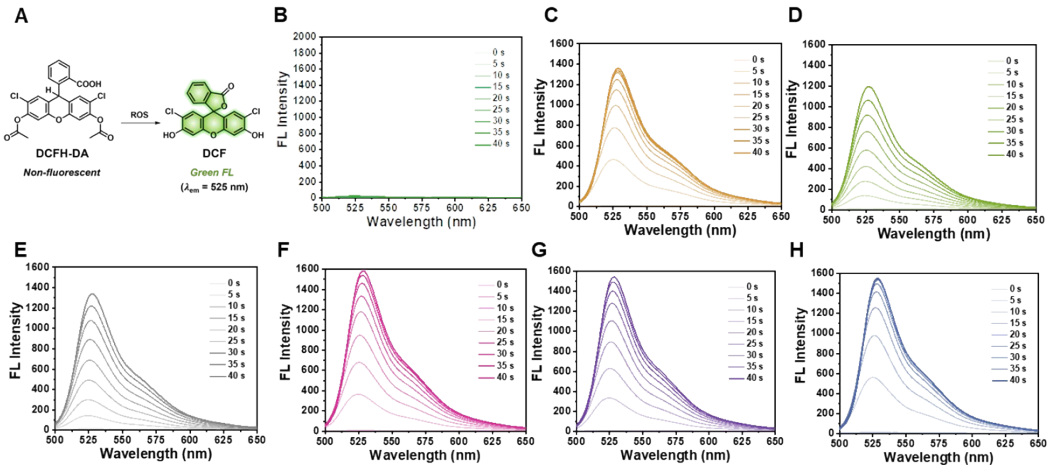

Figure S24. (A) DCFH assays for ROS generation. The fluorescence intensity of DCFH (10 μM) was monitored at 523 nm upon irradiation with a 530 nm PDT Lamp (light intensity of 10 mW cm^{-2}) at 5 s intervals. Each photosensitizer was prepared at a concentration of 5 μM in PBS solution (10 mM, pH 7.4, containing 10% DMSO). The fluorescence intensity ratio (F/F_0) of DCFH at 525 nm was recorded (F_0: each compound's fluorescence intensity of DCFH at 0 s). Fluorescence spectra are shown for (B) DCFH only, (C) BDP-I_2, (D) BDP-Br_2, (E) **Cbz-Bth-BDP**, (F) **DP-Bth-BDP**, and (G) **TPA-th-BDP**.

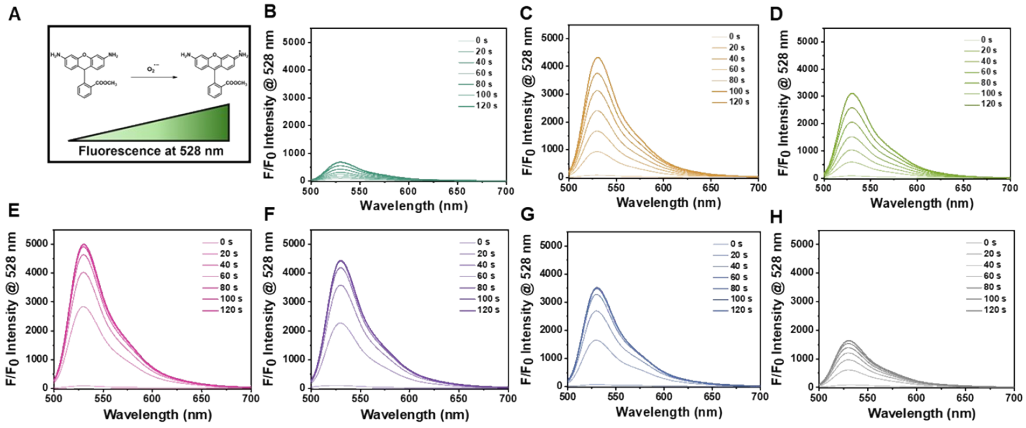

Figure S25. (A) DHR123 assays for superoxide radicals ($O_2^{\bullet-}$) generation. The fluorescence intensity of DHR123 (10 μM) was measured at 528 nm upon irradiation with a 530 nm PDT Lamp (100 mW cm^{-2}) at 20 s intervals. Each photosensitizer (5 μM) was prepared in PBS solution (10 mM, pH 7.4) containing 10% DMSO. The fluorescence intensity ratio (F/F_0) of DHR123 at 528 nm was recorded (F_0: each compound's fluorescence intensity of DHR123 at 0 s). Fluorescence spectra are shown for (B) DHR123 only, (C) BDP-I_2, (D) BDP-Br_2, (E) **Cbz-Bth-BDP**, (F) **DP-Bth-BDP**, (G) **TPA-th-BDP**, and (H) TPA-BDP.

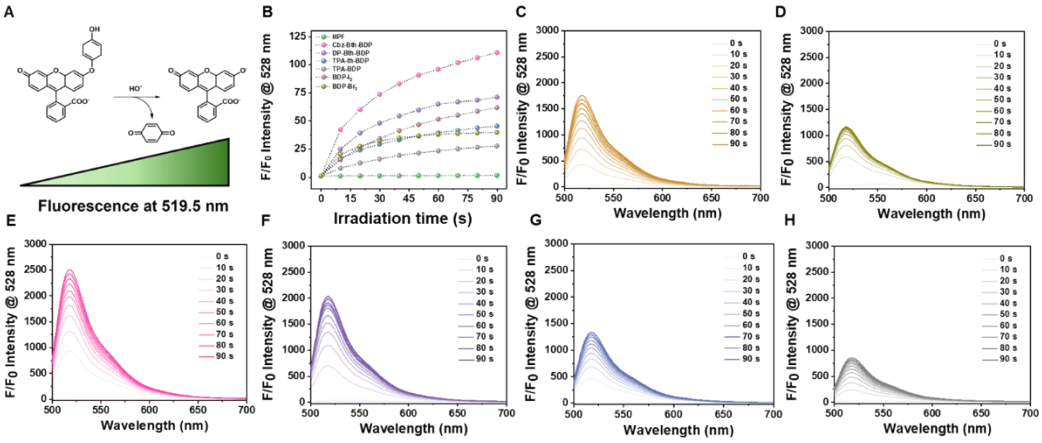

Figure S26. (A) HPF assays for hydroxyl radicals (•OH) generation. The fluorescence intensity of HPF (10 μM) was measured at 528 nm upon irradiation with a 530 nm PDT Lamp (100 mW cm^{-2}) at 10 s intervals. Each photosensitizer (5 μM) was prepared in PBS buffer (10 mM, pH 7.4) containing 10% DMSO. The fluorescence intensity ratio (F/F_0) of HPF at 528 nm was recorded (F_0: each compound's fluorescence intensity of HPF at 0 s). Fluorescence spectra are shown for (B) Comparison of singlet oxygen generation by BODIPY-based photosensitizers, (C) BDP-I_2, (D) BDP-Br_2, (E) **Cbz-Bth-BDP**, (F) **DP-Bth-BDP**, (G) **TPA-th-BDP**, and (H) TPA-BDP.

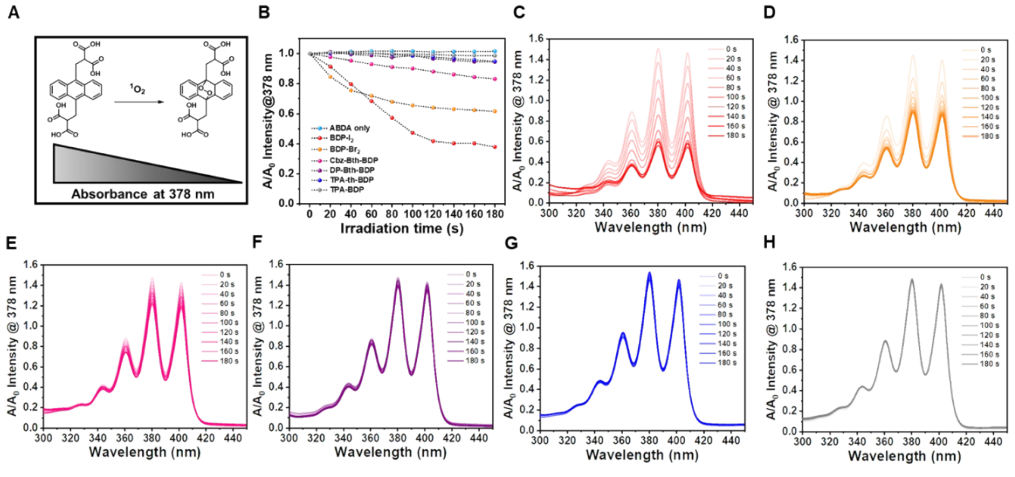

Figure S27. ABDA assay for singlet oxygen ($^1O_2$) generation. The fluorescence intensity of DHR123 (10 μM) was measured at 528 nm upon irradiation with a 530 nm PDT Lamp (100 mW cm^{-2}) at 10 s intervals. Each photosensitizer (5 μM) was prepared in PBS buffer (10 mM, pH 7.4) containing 10% DMSO. (A) The absorbance ratio (A/A_0) of ABDA at 378 nm was recorded (A_0: each compound's absorbance of ABDA at 0 s). Absorbance spectra are shown for (B) Comparison of singlet oxygen generation by BODIPY PCs, (C) BDP-I_2, (D) BDP-Br_2, (E) **Cbz-Bth-BDP**, (F) **DP-Bth-BDP**, (G) **TPA-th-BDP**, and (H) TPA-BDP.

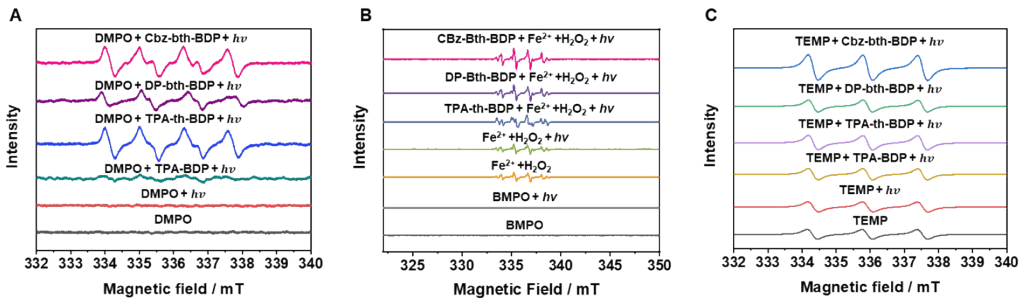

498

499 **Figure S28**. EPR spectra of (A) DMPO (superoxide radical trap, 50 μL mL^{-1}), (B) BMPO (hydroxyl
500 radical trap, 50 μL mL^{-1}), and (C) TEMP (singlet oxygen trap, 50 μL mL^{-1}) were used to assess ROS
501 generation by photo-irradiated thiophene-bridged BODIPY-based photosensitizers. Experiments were
502 performed in DMF, ACN, and DW solutions, respectively. Conditions: 530 nm green light; power
503 density: 100 mW cm^{-2}; irradiation time: 3 min. The concentration of radical trapping agents: 200 μM.
504

505

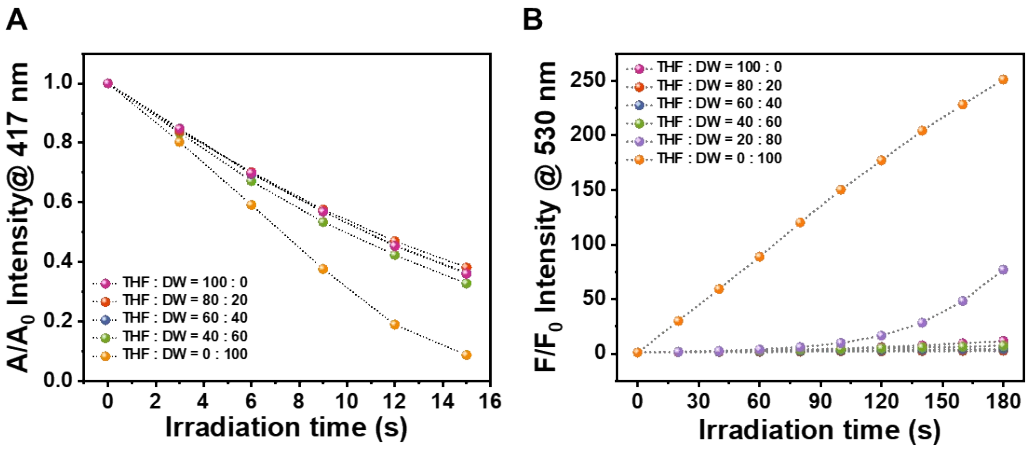

506

507 **Figure S29**. ROS assays in aqueous solutions with varying fractions of THF to investigate the role of
508 aggregation. (A) Degradation rates of DPBF by photoexcited **CBz-Bth-BDP** in THF/water solvent
509 systems. A_0 and A are the absorbance of DPBF at 417 nm before and after irradiation, respectively.
510 (B) DHR123 assays in THF/water mixture by photoexcited **CBz-Bth-BDP**. The fluorescence intensity
511 of DHR123 (10 μM) was measured upon irradiation with a 530 nm PDT Lamp (100 mW cm^{-2}) at 20
512 s intervals. The fluorescence intensity ratio (F/F_0) of DHR123 at 530 nm was recorded (F_0: each
513 compound's fluorescence intensity of DHR123 at 0 s).

514

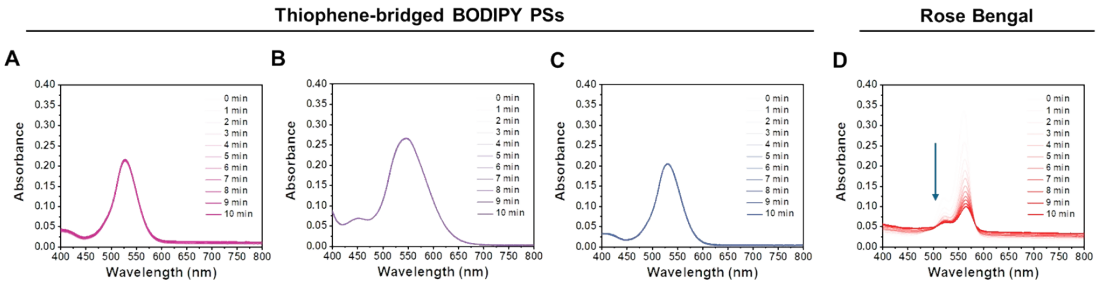

Figure S30. Photostability tests of BODIPY PSs (5 uM) in DCM solution under light irradiation (Irradiation time: 1 min interval, irradiation condition: 530 nm PDT Lamp, 100 mW cm^{-2}). Photostability was detected by using a UV-Vis spectrometer. Absorbance changes of (A) **Cbz-Bth-BDP**, (B)**DP-Bth-BDP**, (C) **TPA-th-BDP**, and (D) Rose Bengal (RB).

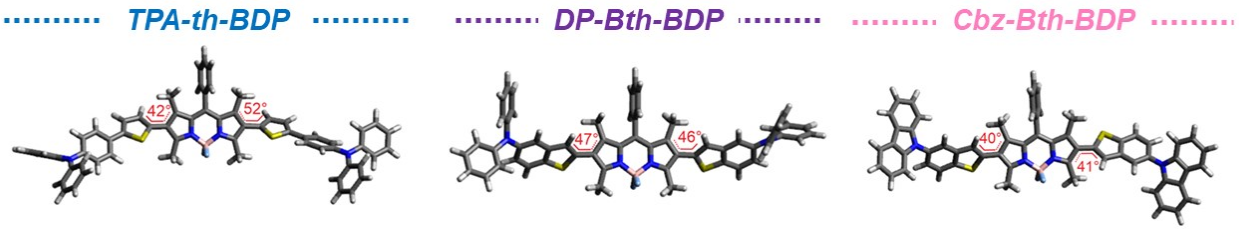

Figure S31. Optimized ground state geometries of **TPA-th-BDP**, **DP-Bth-BDP**, and **Cbz-Bth-BDP** in water, with the dihedral angles of the 2 and 6-substituents highlighted in the insets.

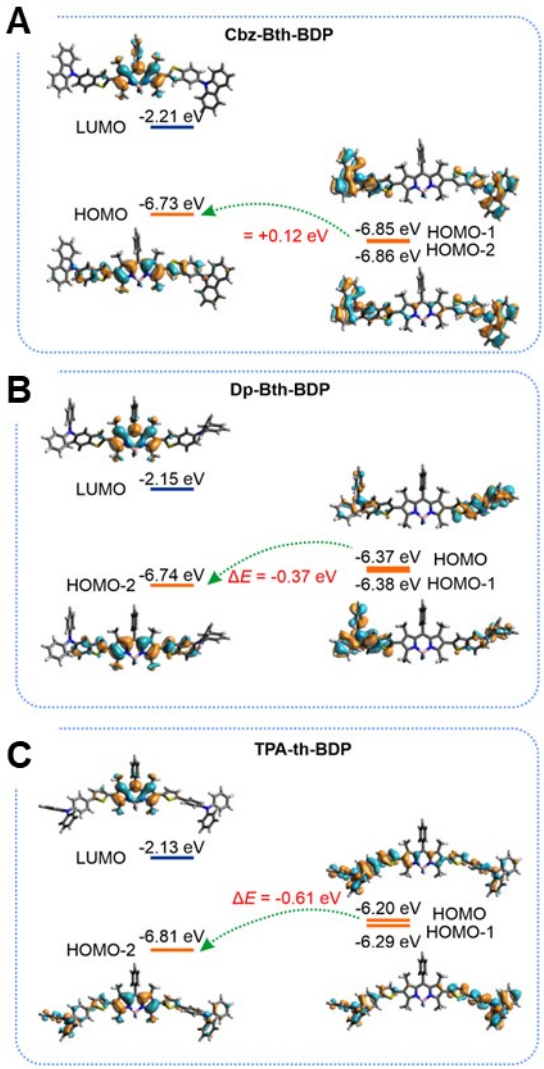

Figure S32. Frontier molecular orbitals (FMO) and their energy levels for (A) **Cbz-Bth-BDP,** (B) **DP-Bth-BDP**, and (C) **TPA-th-BDP**, based on the optimized ground state geometries in water. Note that the plotted energy levels are not to scale for clarity.

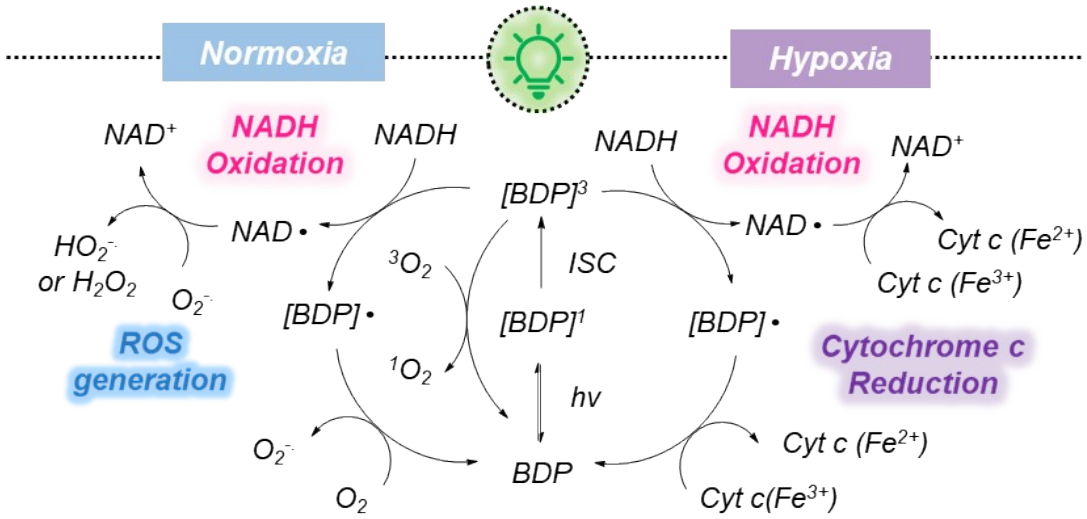

533

534 **Figure S33**. A plausible mechanism of **Cbz-Bth-BDP**-mediated NADH photooxidation and Cyt c
535 reduction.

536

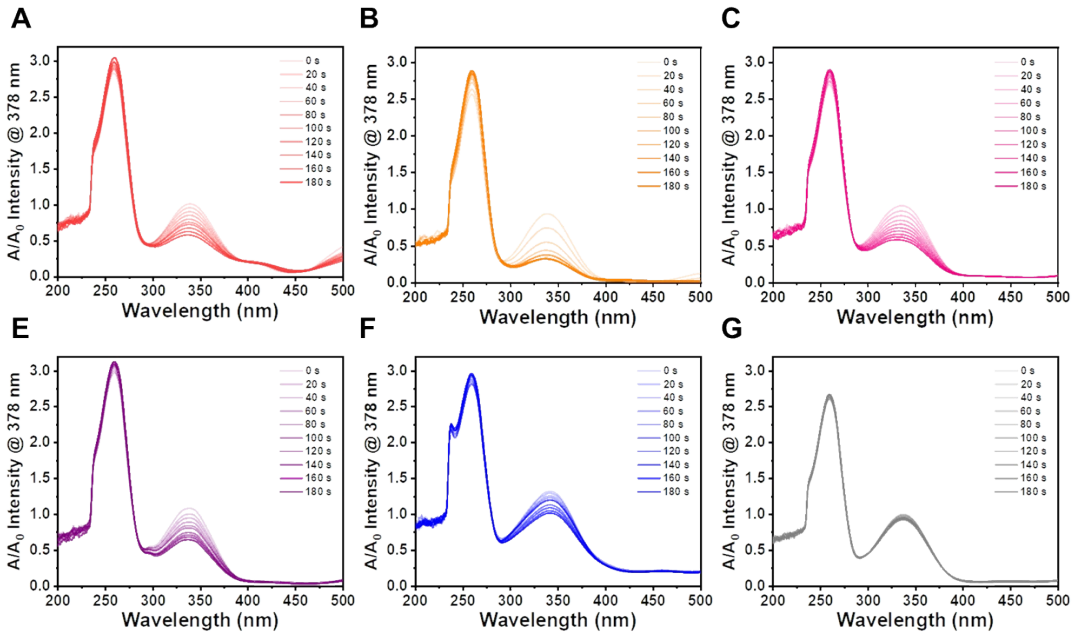

537

538 **Figure S34**. Photocatalytic NADH oxidation. The photosensitizers (5 μM) were irradiated with a 530
539 nm PDT Lamp (100 mW cm^{-2}) from 0 to 180 s, with measurements taken at 20s time interval. NADH
540 was used at 180 μM. NADH (180 μM) oxidation was monitored by the decrease in absorbance at 339
541 nm, indicating its conversion to NAD$^+$. Absorbance spectra are shown for: (A) BDP-I_2, (B) BDP-Br_2,
542 (C) **Cbz-Bth-BDP**, (D) **DP-Bth-BDP**, (E) **TPA-th-BDP**, and (F) TPA-BDP.

543

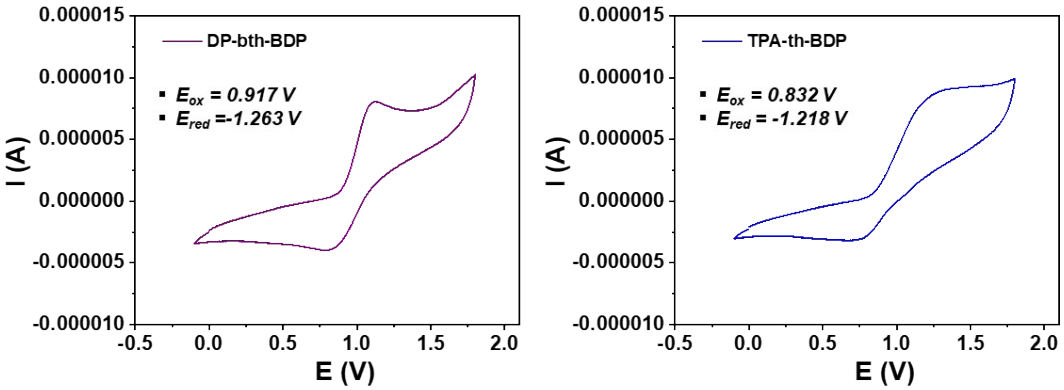

Figure S35. Cyclic voltammetry (CV) measurements of **DP-Bth-BDP** (left) and **TPA-th-BDP** (right).

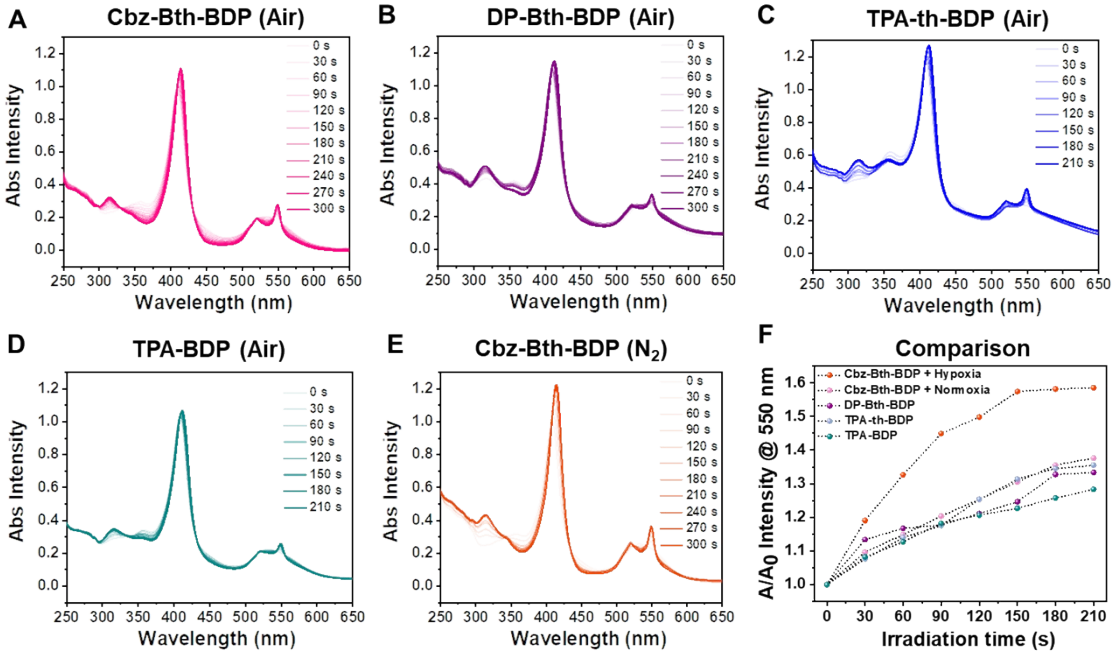

Figure S36. Comparison of **BODIPY**-based photosensitizers-mediated cyt *c* photoreduction efficiency. The appearance of new spectral peaks at the β band (520 nm) and the α band (550 nm) — two characteristic spectroscopic signatures of reduced Cyt *c* (Fe^{2+}) — indicates the photoreduction of Cyt *c* (Fe^{3+}) to (Fe^{2+}). (A-D) Absorbance spectra of cyt c upon photoirradiation with (A) **Cbz-Bth-BDP**, (B) **DP-Bth-BDP**, (C) **TAP-th-BDP**, and (D) TPA-BDP in aerobic conditions (Air). (E) Absorbance spectra of cyt c after photoirradiation with **Cbz-Bth-BDP** in nitrogen (N_2) under green light. All photosensitizers were used at a concentration of 2 μM, with NADH at 40 μM, and cyt c at 10 μM in aerobic PBS solution. (F) Total comparison of BODIPY PSs-mediated Cyt *c* photoreduction efficiency.

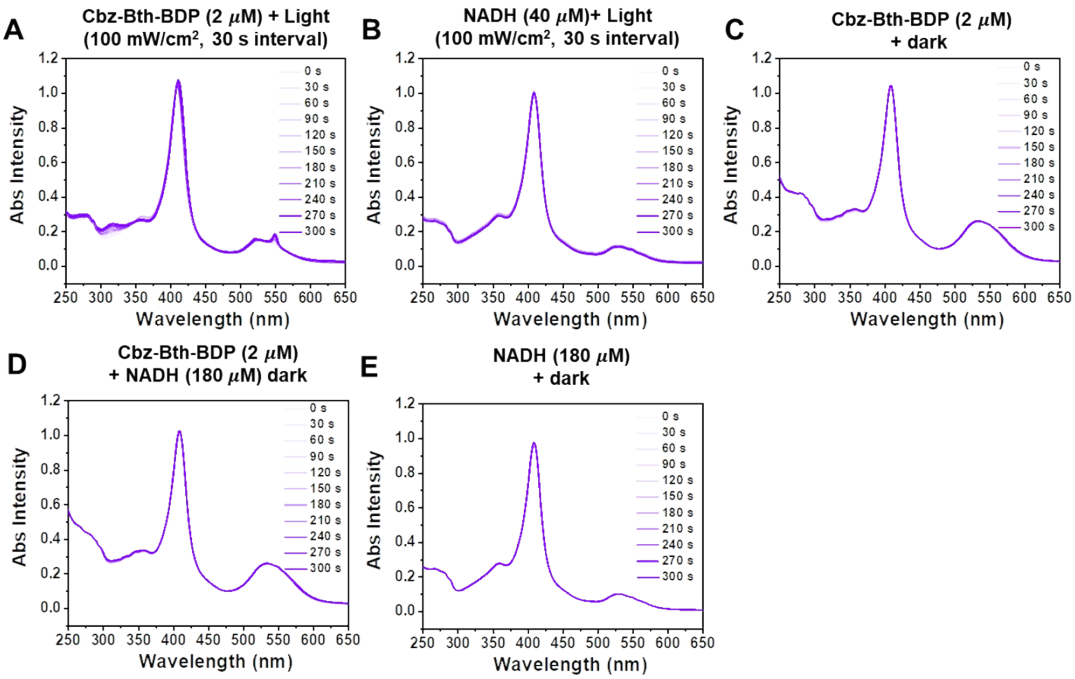

558

559 **Figure S37**. Photocatalytic reduction of Cyt *c* (Fe^{3+}) in the presence and absence of NADH.

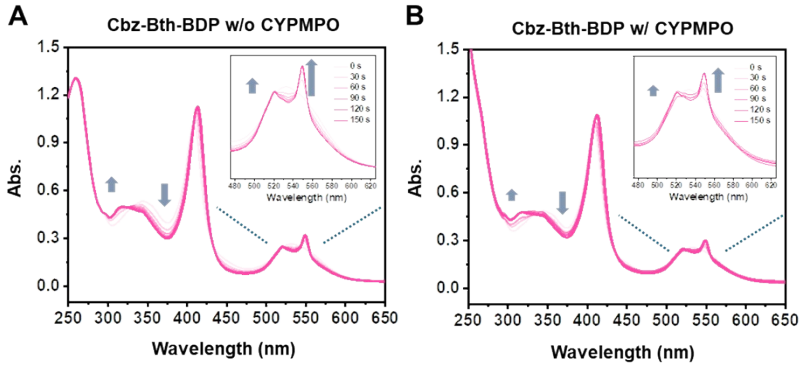

560

561 **Figure S38.** Photocatalytic reduction of Cyt *c* (Fe^{3+}) in (A) the absence or (B) the presence of NAD
562 radical trapping reagent (CYPMPO).

	TON	TOF (min^{-1})
Hypoxia	2.931	0.5862
Normoxia	2.2675	0.4535

563

564 **Figure S39**. Calculation of TON and TOF

565

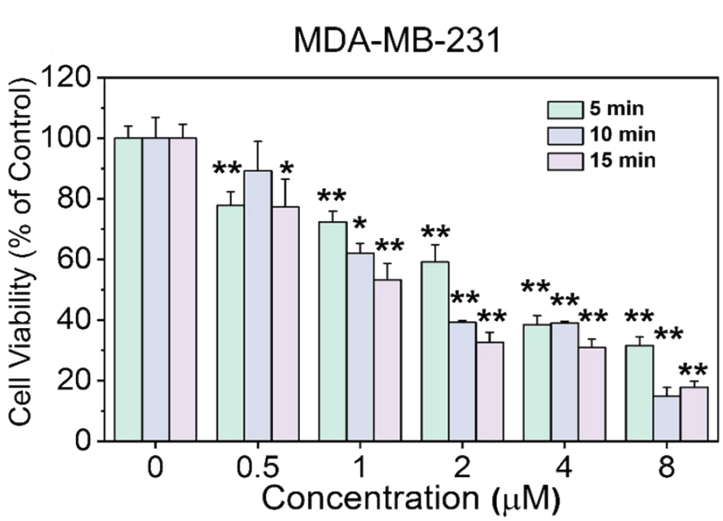

Figure S40. (a) Comparison of cell viability at three different time points (5, 10, and 15 min) after treatment with **Cbz-Bth-BDP** at various concentrations (0, 0.5, 1, 2, 4, and 8 μM) and followed by photo-irradiation. Light power density: 100 mW cm^{-2}, irradiation time: 10 min. Bar graphs represent the mean cell viability from MTT assays, with error bars indicating standard deviation (SD) values (n = 3). *p <0.05, ** p < 0.01, and ***p < 0.001.

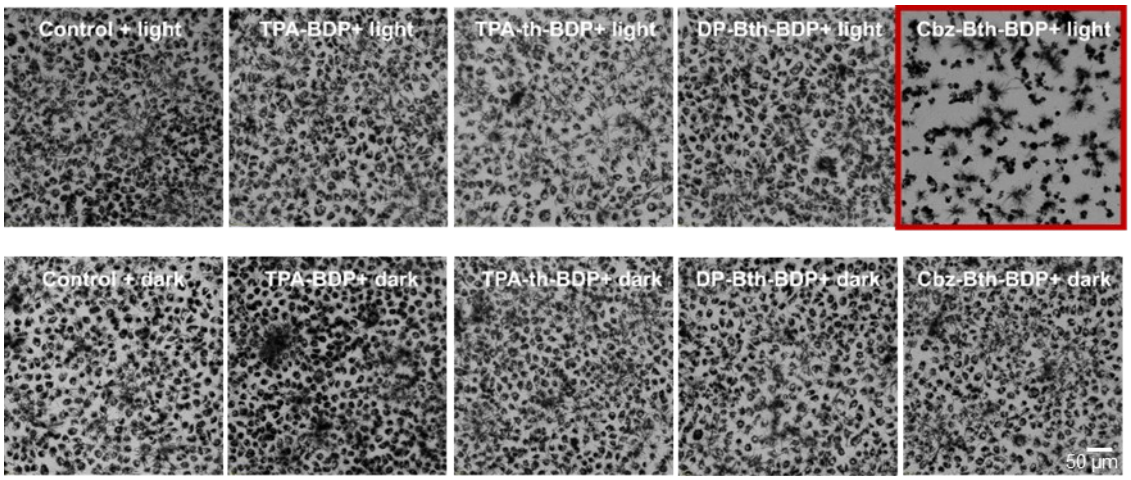

Figure S41. Formazan formation assay in MDA-MB-231 cells with or without light irradiation. MDA-MB-231 cells were treated with 2 μM of indicated concentrations of heavy-atom-free BODIPY PSs (TPA-BDP, **TPA-th-BDP**, **DP-Bth-BDP**, and **Cbz-Bth-BDP**). The formation of formazan was detected using an MTT assay. Three independent experimental runs yielded comparable findings. Scale bar: 50 μm.

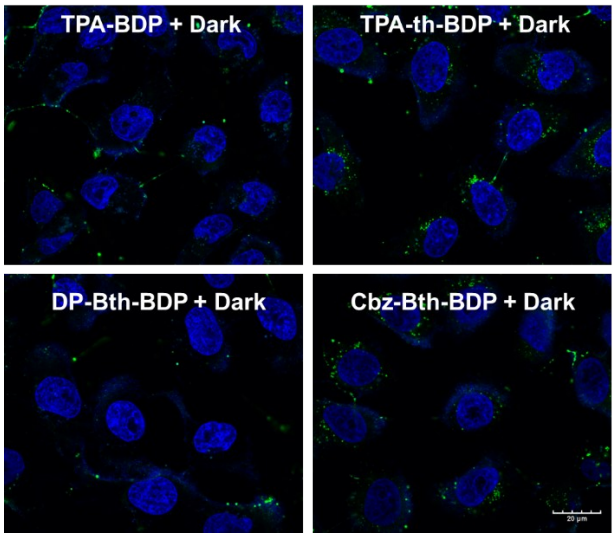

Figure S42. Confocal laser microscopy images showing the pyroptotic morphology changes in MDA-MB-231 cells. The cell membrane is stained with FITC-Annexin-V (green), and the nucleus is stained with Hoechst 33342 (blue). Scale bar: 20 μm.

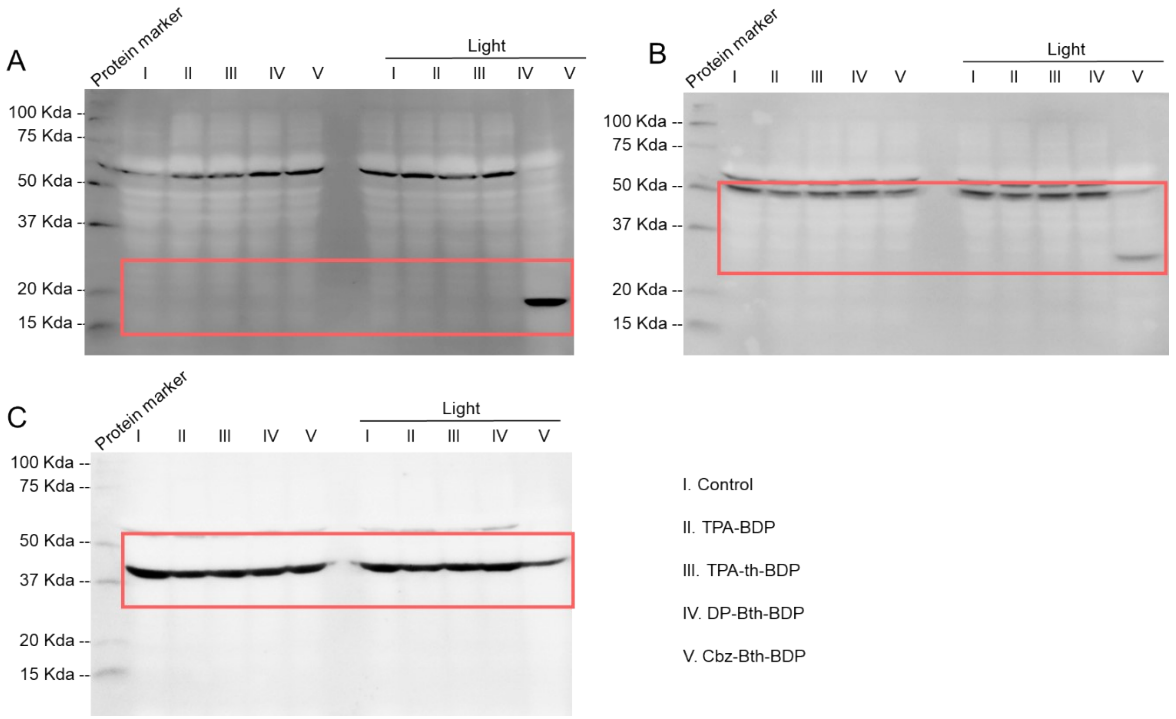

Figure S43. Western blot analysis of pyroptosis-related protein expression levels in MDA-MB-231 cells treated with BODIPY PSs and light irradiation (530 nm, 100 mW cm^{-2}, 10 min). (A) Protein expression of cleaved Caspase-3 (active form of caspase 3). (B) Protein expression of GSDME-N (N-terminal fragment of gasdermin E, GSDME). (C) Protein expression of β-actin.

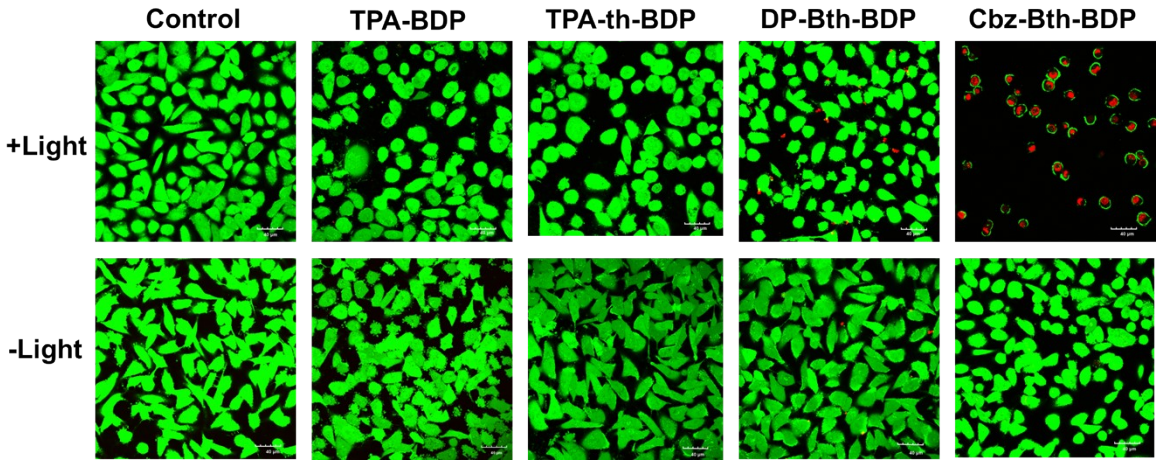

Figure S44. Confocal imaging of live/dead cells in MDA-MB-231 cells. Cells were treated with 2 μM heavy-atom-free BODIP PSs (TPA-BDP, **TPA-th-BDP**, **DP-Bth-BDP**, and **Cbz-Bth-BDP**) with or without light irradiation. Live cells were stained in green by Calcein AM (green, λ_{ex} = 473 nm and λ_{em} = 490-590 nm), and dead cells were stained with propidium iodide (PI) (red, λ_{ex} = 559 nm and λ_{em} = 575-675 nm). Scale bars: 50 μm.

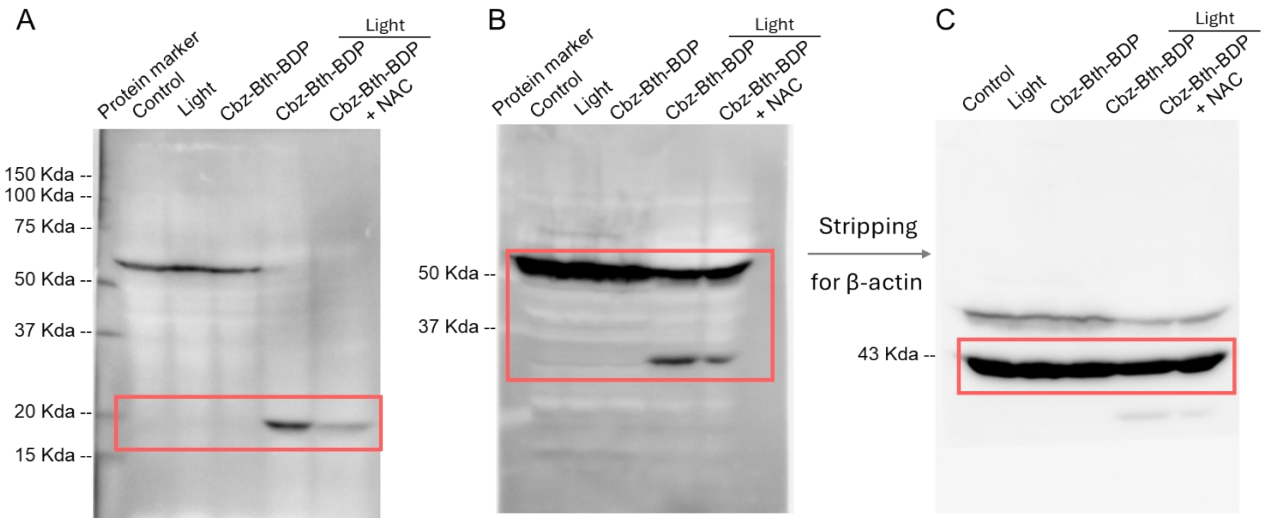

Figure S45. Western blot assay showing pyroptosis-related protein expression after scavenging ROS (N-Acetyl-L-cysteine, NAC) with Cbz-Bth-BDP treatment. (A) Protein expression of cleaved Caspase-3 (active form of caspase 3). (B) Protein expression of GSDME-N (N-terminal fragment of gasdermin E, GSDME) was analyzed, after which the membrane was stripped and reprobed for β-actin (C). Light irradiation condition: 530 nm, 100 mW cm^{-2}, 10 min.

Supplementary Reference

[1] J. Wei, Y. Ma, C. Liu, J. Li, J. Shen, K. Y. Zhang, S. Liu, Q. Zhao, *J. Mater. Chem. C* **2021**, *9*, 5945–5951.

[2] I. Partanen, A. Belyaev, B. Su, Z. Liu, J. J. Saarinen, I. Ibni Hashim, A. Steffen, P. Chou, C. Romero-Nieto, I. O. Koshevoy, *Chem. Eur. J.* **2023**, *29*, e202301073.

[3] F.-Z. Xu, L. Zhu, H.-H. Han, J.-W. Zou, Y. Zang, J. Li, T. D. James, X.-P. He, C.-Y. Wang, *Chem. Sci.* **2022**, *13*, 9373–9380.

[4] Y. Peng, G. Guo, S. Guo, L. Kong, T. Lu, Z. Zhang, *Angew. Chem. Int. Ed.* **2021**, *60*, 22062–22069.

[5] V. Nguyen, Y. Yim, S. Kim, B. Ryu, K. M. K. Swamy, G. Kim, N. Kwon, C. Kim, S. Park, J. Yoon, *Angew. Chem. Int. Ed.* **2020**, *59*, 8957–8962.

[6] K. Teng, W. Chen, L. Niu, W. Fang, G. Cui, Q. Yang, *Angew. Chem. Int. Ed.* **2021**, *60*, 19912–19920.

[7] M. D. Hanwell, D. E. Curtis, D. C. Lonie, T. Vandermeersch, E. Zurek, G. R. Hutchison, *J. Cheminform.* **2012**, *4*, 17.

[8] A. V. Marenich, C. J. Cramer, D. G. Truhlar, *J. Phys. Chem. B* **2009**, *113*, 6378–6396.

[9] F. Neese, *WIREs: Comput. Mol. Sci.* **2022**, *12*, e1606.